UNIVERSIDADE D
COIMBRA

Ana Filipa Borges Cortês

Mechanisms of high-level perceptual decision: a neuroscientific approach

Dissertation submitted to the Faculty of Science and Technology of the University of Coimbra for the degree of Master in Biomedical Engineering with specialization in Neurosciences, supervised by Professor Miguel Castelo-Branco and PhD João Valente Duarte.

September 2022

Mechanisms of high-level perceptual decision: a neuroscientific approach

Ana Filipa Borges Cortês

Supervisors:
Professor Miguel Castelo-Branco
PhD João Valente Duarte

Coimbra, September 2022

This work was developed in collaboration with:

ICNAS – Institute for Nuclear Sciences Applied to Health

CIBIT – Coimbra Institute for Biomedical Imaging and Translational Research

FCT - Portuguese Foundation for Science and Technology

Agradecimentos

Este trabalho foi desenvolvido com o apoio da Fundação para a Ciência e Tecnologia (FCT) através do projeto Neural mechanisms underlying positive and negative perceptual hysteresis (PTDC/PSI-GER/1326/2020) e do financiamento estratégico institucional ao CIBIT (FCT/UIDB/4950 e FCT/UIDP/4950).

Esta dissertação marca o encerrar de um capítulo. Foram cinco anos de muitas aprendizagens, trabalho e crescimento, e não posso deixar de agradecer profundamente a todos aqueles que apoiaram esta caminhada, em especial:

Aos meus orientadores, Professor Doutor Miguel Castelo-Branco e Doutor João Valente Duarte, por tudo o que me ensinaram, pela disponibilidade, empenho e dedicação a este projeto.

Ao ICNAS e ao CIBIT, e a todos os seus elementos que contribuíram para a realização deste trabalho.

A todos os voluntários que aceitaram participar neste projeto.

Aos meus amigos, em particular, à Margarida, à Rute, à Ulyana, ao Telmo e à Beatriz, pelo apoio incondicional, pela companhia em sessões de estudo e por todas as divertidas memórias criadas durante esta caminhada.

À Beatriz Martinho por todo o carinho e conselhos ao longo destes cinco anos.

Aos meus tios, Eduardo e Anabela, por tudo o que aprendi e aprendo com eles.

À minha madrinha, Margarida, pelo apoio e carinho sempre presentes.

À minha avó Maria, e aos meus avós, Alice e António, por todo o carinho, paciência e aprendizagens.

À minha irmã, Andreia, por ser a minha conselheira e por acreditar sempre em mim.

À minha mãe, Isabel, e ao meu pai, António, por tudo o que fizeram e fazem todos os dias por mim, pelo amor e confiança que sempre estiveram presentes. Por serem o meu refúgio. Sem vocês nada disto era possível.

A todos o meu sincero obrigada!

Abstract

Perceptual decision can be defined as the process in which the sensory information retrieved and processed in the brain is used to define actions towards the external environment. It is strongly influenced by bottom-up factors, such as the sensory information, as well as top-down factors, including previous experiences, culture, and emotion. The mechanisms underlying this process have been extensively studied but are yet to be fully understood.

Hysteresis is a well-known phenomenon in physics, that has been raising substantial neuroscientific interest, to describe the influence of perceptual history in decision-making. It manifests itself through two different mechanisms: persistence, or positive hysteresis, causing a positive lag in the change of perception, and adaptation, or negative hysteresis, the cause of a negative lag in the change of perception.

This project tested the hypothesis that there is hysteresis, positive and/or negative, in the perception of emotion in biological motion patterns, which is the understanding and processing of human motion patterns, conveying happiness or sadness, using stimulus that required emotion recognition through these patterns. Our main hypothesis is that these two mechanisms, positive and negative hysteresis, compete to influence the perception of biological motion conveying either happy or sad emotional content.

We used both a behavioural assessment, through the realization of a psychophysics experiment, as well as a functional magnetic resonance imaging (fMRI) experiment to study the neural correlates of hysteresis phenomena.

Behavioural assessment revealed the existence of hysteresis in perception of happy or sad biological motion patterns, with a predominance of positive hysteresis but a significant contribution of negative hysteresis to perception. Therefore, it seems that there is in fact a competitive balance between both mechanisms in the perceptual decision-making. We also present preliminary fMRI results regarding the neural correlates of these mechanisms.

Keywords: Hysteresis; Biological motion; Perceptual decision; Neuroimaging

Resumo

Decisão percetual pode ser definida como o processo através do qual a informação sensorial que é recebida e processada pelo cérebro pode ser usada para definir ações em relação ao ambiente externo. Este processo é fortemente influenciado por fatores *bottom-up*, como a informação sensorial, bem como por fatores *top-down*, que incluem experiências anteriores, aspetos culturais de alto nível e as emoções. Os mecanismos subjacentes a este processo têm sido extensivamente estudados, mas não são ainda inteiramente conhecidos.

A histerese é um fenómeno bem-conhecido na física, e que tem emergido também em estudos neurocientíficos como forma de descrever a influência da história na tomada de decisões, manifestando-se sob a forma de dois mecanismos distintos: a persistência, ou histerese positiva, que causa um desfasamento positivo na mudança de perceção, e adaptação, ou histerese negativa, que causa um desfasamento negativo na mudança de perceção.

Este projeto testa a hipótese de que existe histerese, positiva e/ou negativa, na perceção de emoções a partir do movimento biológico, isto é, no processamento e compreensão dos padrões de movimento humano, transmitindo emoção feliz ou triste, usando estímulos que requerem reconhecimento emocional com base nestes padrões. A nossa principal teoria é de que estes dois mecanismos, histerese positiva e negativa, competem para influenciar a perceção de movimento biológico transmitindo emoção feliz ou triste.

Para estudar esta teoria, efetuámos um estudo comportamental, com a realização de uma experiência de psicofísica, bem como estudos de imagem por ressonância magnética funcional para estudar os correlatos neurais envolvidos no fenómeno de histerese.

O estudo comportamental revelou a existência de histerese na perceção do comportamento biológico transmitindo emoção feliz ou triste, com predominância da histerese positiva mas com uma contribuição significativa de histerese negativa. Assim, parece de facto que existe um balanço competitivo entre ambos os mecanismos na decisão percetual. Apresentamos ainda, nesta dissertação, resultados preliminares acerca dos correlatos neuronais responsáveis por estes mecanismos com base nos primeiros dados recolhidos usando ressonância magnética funcional.

Palavras-chave: Histerese; Movimento Biológico; Decisão percetual; Neuroimagem

List of Abbreviations and Acronyms

ACC - anterior cingulate cortex
aIPS – anterior intraparietal sulcus
BOLD - blood oxygenation level-dependent
CSF - cerebrospinal fluid
DLPFC - dorsolateral prefrontal cortex
DMN - default mode network
EBA - extrastriate body area
EPI - echo planar imaging
FA – flip angle
FBA - fusiform body area
FEF - frontal eye fields
FFA – fusiform face area
FFG - fusiform gyrus
FFX – fixed-effects analysis
fMRI - functional Magnetic Resonance Imaging
FOV – field of view
GLM – general linear model
HRF – hemodynamic response function
IFG - inferior frontal gyrus
IPL - inferior parietal lobe
IPS - intraparietal sulcus
IT - inferior temporal cortex
LGN - lateral geniculate nucleus
MR – magnetic resonance
MRI - magnetic resonance imaging
MST - medial superior temporal area
MT – middle temporal area
N – null
NH – negative hysteresis
OFC - orbitofrontal cortex
PCA - principal components analysis
PCC - posterior cingulate cortex
PFC – prefrontal cortex
PH – positive hysteresis
PLD – point-light display
PLW – point-light walker
PMd - dorsal premotor cortex
pmPFC - posterior medial prefrontal cortex
PPA - parahippocampal place area
RF - radiofrequency
SMA - supplementary motor area
SPL - superior parietal lobe
STS - superior temporal sulcus
TE – echo time
TPJ - temporoparietal junction
TR – repetition time
UN – undefined
vPMC - ventromedial prefrontal cortex

List of Figures

List of Tables

Contents

Chapter 1. Theoretical Background

1.1. Motivation and Objectives

In our daily lives, we are constantly making decisions based on the information retrieved by the sensory systems. The process of receiving this information and translating it into behaviour, either by planning actions or making judgements, is designated as perceptual decision. The mechanisms underlying this phenomenon are yet to be fully decoded.

It is known that perceptual decision is influenced by both top-down factors, such as previous experiences, culture, emotion, and motivation, as well as bottom-up factors, which include the sensory stimulation, such as visual input.

Visual adaptation occurs when the visual system changes its operating properties in response to the stimuli it receives from the surrounding environment. The processes based on this phenomenon have been well studied in the motion domain. Neural responses to visual global motion maps on the visual dorsal stream, particularly in the area V5/MT. Neural selectivity has been studied using adaptation-based paradigms and fMRI.[1]–[4]

Paradigms of prolonged adaptation to motion, such as drifting gratings, can cause an alteration in the visual system, such that the response in V5/MT decreases despite continuous stimulation. On the other hand, high-level mechanisms of attention and memory contribute to maintenance of the current perception, which we can define as persistence.

If adaptation is sufficiently prolonged neural fatigue occurs and the current percept tends to fade, which cannot be overridden even by the high-level mechanisms of attention and memory. The main hypothesis of this project is that two neural processes compete in the perception decision making: adaptation and persistence.

In a situation in which the visual system has to decide between two different interpretations, adaptation is a cause of negative hysteresis which favours the change into the competing perception earlier, causing a negative lag. Persistence, which is caused by

short-term memory processes, is a cause of positive hysteresis in which the current perception is maintained for a longer period of time, causing a positive lag.

The objectives of this project are, therefore, to understand the general and domain-specific mechanisms in the dynamics of perceptual decision-making and learning, and to study the low and high-level mechanisms involved in perceptual hysteresis, using a biological motion stimulus containing emotional patterns of motion paired with an emotional recognition task.

Understanding the neurobiological underpinnings of perceptual decision making and learning can be relevant for the understanding of diseases characterized by alterations in perceptual states, such as autism spectrum disorder.

In this project, we study the neural correlates underlying these mechanisms and the hypothesis of their competitive balance, by combining behavioural assessment with fMRI.

1.2. Perceptual Decision

Perceptual decision can be described as the process in which the brain translates the sensory inputs into actions and judgements and therefore, being central to regulate behaviour.[5]

Given its importance to the understanding of the cognitive function and behaviour, multiple studies have been performed focusing on the understanding of this process and progress has been made regarding the specification of brain areas involved in it. Current literature has established decision-making as a process that engages several areas across the entire brain to perform the different steps necessary such as the receiving of sensory information, the processing of this information, the planning of actions and their execution. [6]

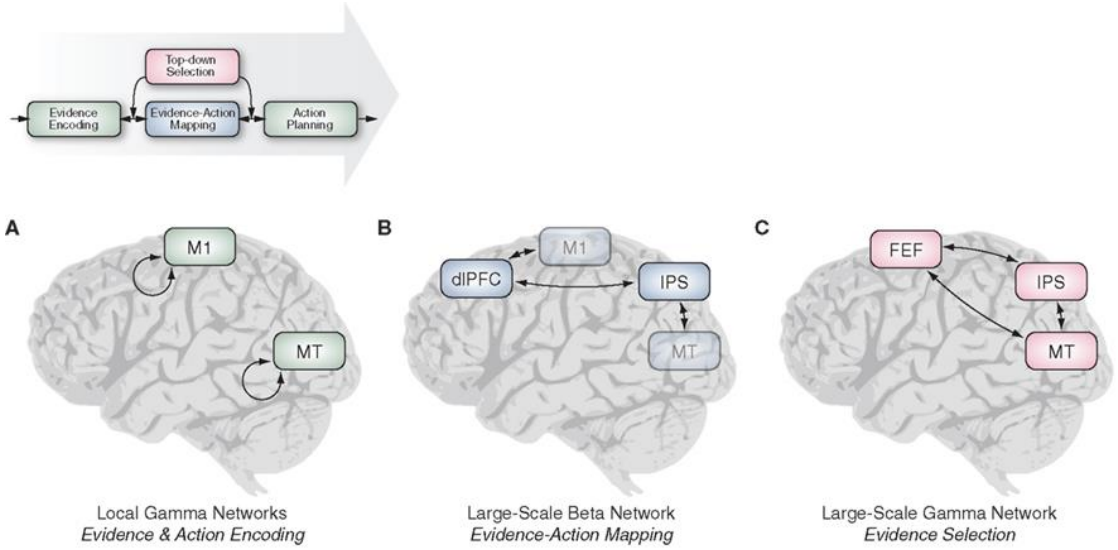

Figure 1. Schematic representation of the areas involved in decision-making studies using motion stimuli: middle temporal area (MT), motor cortex (M1), dorsolateral prefrontal cortex (dlPFC), intraparietal sulcus (IPS), and, frontal eye fields (FEF). Source:[6].

The sensory evidence is represented in different brain areas according to the category of the information received. For example, tactile information seems to be processed in the somatosensory cortex while face representations are perceived in the fusiform face area (FFA), emotional expressions in superior temporal sulcus (STS) and houses/scenes in the parahippocampal place area (PPA). The left posterior dorsolateral prefrontal cortex (DLPFC) has also been linked to the perceptual decision-making as an area that integrates the information from the different sensory areas to create a representation of the sensory information overall.[7]–[10] The medial frontal gyrus has also been thought to have a role in comparing stimulus to categorical boundaries while the Middle Temporal area (MT) as well as the motor cortex present a role linked to visuomotor integration, by processing visual motion stimuli that is then used in further steps of decision-making and action planning and execution.[6]

Perceptual decision is not only influenced by the sensory inputs that reach the brain but also by the attention and task difficulty. In fact, task difficulty appears to be correlated with response time and consequently with the level of activation of the brain areas, with more difficult tasks evoking greater responses. [5], [10]–[12] Insula, the inferior frontal gyrus (IFG) and the anterior cingulate cortex (ACC) are areas that have been mentioned in several studies for having a positive correlation with the response times. [11], [13]

Intraparietal sulcus (IPS), the frontal eye fields (FEF), and the dorsal premotor cortex (PMd) have been linked to the planning of decision-reporting actions, with IPS and FEF presenting stronger activations during the periods of decision formation. [14]–[18]

Independently of the action that comes as an output of the decision-making, the process itself seems to engage four particular areas: the left posterior DLPFC, the left posterior cingulate cortex (PCC), the left IPS and the left fusiform gyrus. [19] The posterior DLPFC seems to have a critical role not only in the representation of sensory information but also in the translation of the decision to an action. Brain areas involved in this process are not only responsible for the decision-making and for the planning of the response but also for monitoring the performance and adjusting the activity of the networks according to the outcomes. It seems that the brain adjusts the process by amplifying certain areas, through top-down loops, relevant to the task at hand to better improve the performance. This performance-monitoring system appears to depend strongly on the posterior medial prefrontal cortex (pmPFC). [20]

Despite the number of experiments performed to decipher the mechanisms behind perceptual decision-making, the connections and hierarchy between all the areas that have been shown to be linked to it are still yet to be fully understood.

1.3. Hysteresis

Hysteresis is a phenomenon widely known in physics, particularly in the field of electromagnetism, that describes the dependence of the output of a system on the input of the same system. [21]–[23] Recently, it has been gaining attention in neurosciences, especially in the human vision research. [24]–[27]

Classically hysteresis has been seen as a persistence on maintaining a certain state of the system despite the changes of input, creating a later transition to the other percept in comparison to the control situation, where there is no influence of the history of the system. There is now recent evidence (initially in the field of physics but now also in perceptual science) of the opposite effect: the transition in perception happening before the input changing.[28]–[32] It is therefore now necessary to study and distinguish these two effects. The terminology adopted describes the mechanism of persistence as a

positive hysteresis effect while the anticipation of the perception is attributed to a negative hysteresis effect. [29], [33]

This way, hysteresis can also be described as the competitive balance of two opposing forces, the competing stimulus representation (perceived prior) and the stimulus currently being presented/perceived. The perceptual hysteresis comprises two different neural mechanisms: persistence, which causes positive hysteresis forcing the system to keep the current perception for longer periods of time, and adaptation, a cause of negative hysteresis that favours the switch to the competing perception.

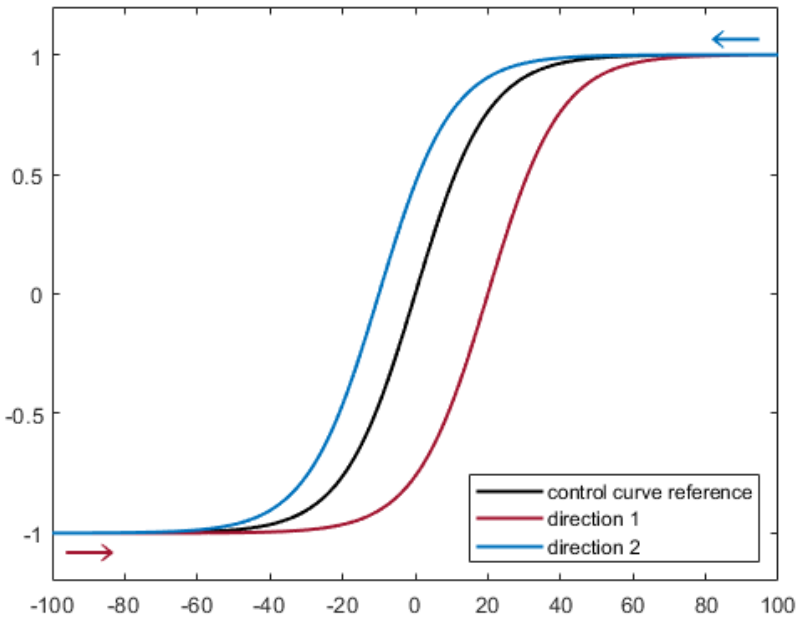

Figure 2. Example of a hysteresis loop following the classical form discovered in physics. In black is the control curve, reflecting what would happen without the effect of the history; in red and blue there are the two directions of the trajectory, starting on the opposite states and ending in the other state.

The human brain seems to retrieve and recycle information and action plans to improve performance while reducing the resources, a process of efficiency optimization, needed for it. Practicing and training a sport, for example, are situations where the effect of the history of the motion patterns previously used manifests itself in improving the performance.

Several studies (see Table 1) have proven the existence of hysteresis in biological motion, that is the motion patterns, regarding actions as catching an object, grasping, pointing, or

opening drawers, in terms of action planning and the execution of the movement itself. [32], [34]–[42] There are strong evidence of the occurrence of hysteresis in these movements as the brain often reuses information regarding previous actions to plan new ones, especially when these are done in sequence.

Table 1. Table synthesis of the studies of hysteresis using biological motion stimuli. The research criteria for this synthesis included only studies in humans, involving muscular movement and actions, and therefore excluding studies at cell and tissue level, and including the terms "motor" and "hysteresis".

Author	Parameter in study and task	Participant group	Results observed	Reference
Lopresti-Goodman *et al.* (2013)	Grasping objects with one or two hands	Healthy adults	Adaptation observed in the choice when presented with an object previously grasped	[32]
Valyear *et al.* (2019)	Hand choice based on a presented target	Healthy adults	Presence of hysteresis: faster responses when choosing the same hand from previous actions; slower responses when choosing the other hand	[34]
Schütz *et al.* (2016, 2017)	Opening a drawer and pointing towards an object	Healthy adults	Persistence on the former posture for both conditions	[35], [36]
Rostoft *et al.* (2002)	Catching a ball based on the location	Healthy 4-year-old children	Presence of hysteresis in the choice of the hand: the switching point from one hand to the other changes with the direction of the trajectory	[37]
Land *et al.* (2013)	Posture when performing the task: walk to a drawer, open it, grasp an object located in different places in different trials.	Healthy adults	The posture adopted was a result of both the anticipation of the task, in particularly, in function of the initial location of the object and the history of the movements. Consistent postures in similar trials with similar tasks	[38]
Weiler *et al.* (2000)	Move from two different positions with the knee joint at different angles (15º and 75º) to a position with the knee joint at a certain target angle (30º,45º and 60º). First the movement is done passively and then the	Healthy adults	Clear effect of the history of the trajectory suggests the presence of hysteresis: moving from a 15º angles towards any of the target positions resulted in lower errors than moving from the 75º angle.	[39]

	participant did it on their own trying to replicate the passive movement.			
Kostyukov *et al.* (2022)	Performing slow circular movements with the right hand holding a moving handle operated by a machine.	Healthy adults	Presence of hysteresis: differences in the elbow muscles regarding the intensity, the muscle length and the force used when comparing the two directions of movement.	[40]
Adhikari *et al.* (2013)	Tap the right index finger on a response box accordingly to the visual cues given.	Healthy adults	Hysteresis effect: the BOLD signal was different in the precuneus when the tapping was in an accelerating phase in comparison to a decelerating phase.	[41]
Burgess-Limerick *et al.* (2001)	Cyclic lifting and lowering task.	Healthy adults	Presence of hysteresis: different movement patterns when changing the starting and ending points.	[42]

Hysteresis not only manifests itself in motor patterns but also in the perception of, for example, visual and auditory stimuli. Among the recent studies of hysteresis in perception, there are few that relate emotion perception to hysteresis (see Table 2).

When we are trying to assess the emotions expressed by those around us, we are constantly looking for visual and auditory clues, like the facial expression, the body language, or the tone of voice. These are factors that change over time as the emotional state is also in constant change. In 1993, Kobayashi and Hara, used human facial expressions to prove that emotion recognition and processing can be interpreted as dynamic systems being that emotions appear and change across time, depending not only on the temporal context but also on the trajectory of the input information, that is, presenting hysteresis. [43]

From the studies performed using a task of emotional recognition, with the exception of one study that used sounds that portrayed emotions and noise [44], all of these use facial expressions to create dynamic transitions to use as stimuli. [29], [44]–[48] Human faces are the part where most of our attention is focused when socializing and the interpretation of the expressions is a necessary skill to survive and thrive in society. Therefore, it is not surprising that the brain has certain areas and networks specialized in the processing of

faces, making this a much faster process to perceive and to plan responses to those, manifesting them either through actions or physiologically, which in turn makes facial expressions very interesting tools to study perceptual mechanisms.[49]

Table 2. Table synthesis of the studies of hysteresis involving the recognition of emotions.

Author	Type of stimulus	Participant group	Results observed	Reference
Webster *et al.* (2004)	Facial expressions	Healthy adults	Negative hysteresis	[45]
Verdade *et al.* (2020, 2022)	Facial expressions	Healthy adults	Positive hysteresis	[46], [47]
Sacharin *et al.* (2012)	Facial expressions	Healthy adults	Predominantly positive hysteresis Negative hysteresis in some directions	[48]
Liaci *et al.* (2018)	Facial expressions	Healthy adults	Positive and negative hysteresis	[29]
Martin *et al.* (2014)	Sounds	Control group of healthy adults Adults with a diagnostic of schizophrenia	Positive hysteresis for both groups in the direction of decreasing of signal-to-noise ratio	[44]

The majority of the studies in emotion perception present a predominance of positive hysteresis, either not observing negative hysteresis or having only very specific directions with those. Similar emotions such as anger and disgust often do not evoke hysteresis and when they do, it is a weaker effect when comparing with pairs of emotion with more distinct differences such as sadness and happiness.[46], [48]

These studies also acknowledge a bias towards happiness with trajectories where this is the first emotion presented having longer periods of persistence and those that start with another emotion having an earlier transition towards the perception of happiness. [46], [48] This observation is in agreement with the theory of the happiness superiority effect. [50]–[52]

Emotion perception is not based solely on analysis of facial expressions, rather it is the product of the integration several types of information such as auditory cues, like the tone of voice and the patterns of speech, as well as body language expressed through posture and motion patterns. In fact, when people are presented with only face expressions partially hidden by face masks, the recognition of emotions decreases significantly, [53] but if the body is also shown there is not a big difference between the recognition of

emotions with or without face masks. This suggests that body language and consequently, biological motion, affects strongly the emotional recognition.[54]

With the strong evidence of hysteresis in the human motor system and the perception of emotion in facial expressions, perceiving emotion from biological motion will likely use the same mechanisms of perception.

Furthermore, the perception of biological motion is often times compromised in neurodevelopmental disorders, such as autism. [55] Understanding the mechanisms in the basis of the perception of these stimuli can be a step towards better understanding these deficits and foster the development of therapies to improve the communication and social skills improving the quality of life of these people.

1.4. The Human Visual System

Visual stimulation is often used in perceptual studies because of the ease of stimulus manipulation and control, as well as because the visual system is probably the best understood sensory system. Furthermore, visual information seems to have a larger impact on emotion perception than auditory stimulation. [56]

Planning and executing perceptual studies using this kind of stimulation require the understanding of the visual system not only to plan the experiment itself but also to generate predictions of evoked neural responses.

The retina is the principal neural structure in the eye that detects light and transmits the information to the other structures of the brain. It is composed by several different layers, and a canonical vertical circuit including the photoreceptors, the bipolar cells, and the ganglion cells. [57]

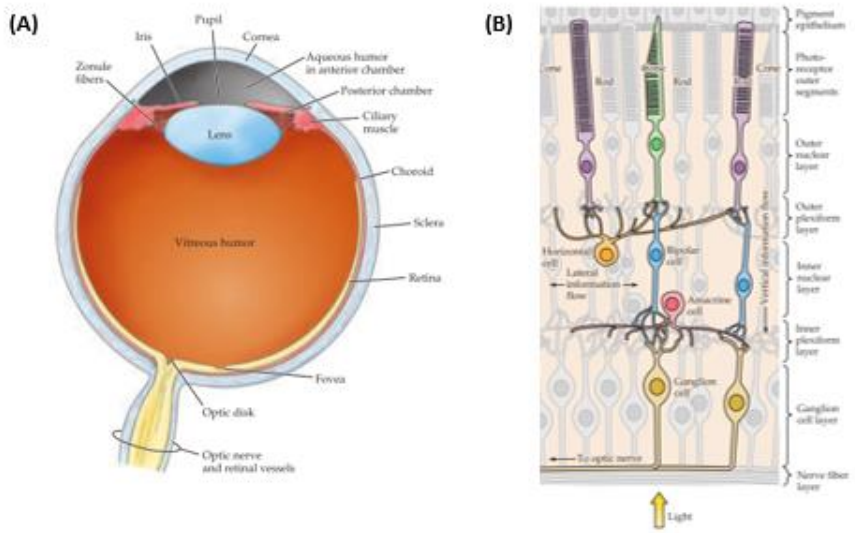

Figure 3. Anatomy of the eye (A) and constitution of the retina of the eye (B). Source: adapted from [57].

The photoreceptors are the cells responsible for the photo transduction which is the process of conversion of the light into electric potentials that are then transmitted to the bipolar cells and then the ganglion cells which will send the information to the brain. The communication between the photoreceptors and the bipolar cells is modulated by the horizontal cells while the communication between the bipolar cells and the ganglion cells is modulated by the amacrine cells. [57]

Visual information collected from the retina is then processed in the thalamus, particularly in the lateral geniculate nucleus (LGN). LGN is constituted by four parvocellular laminae, which constitute the P pathway, and two magnocellular laminae, which constitute the M pathway. Both pathways are processed in parallel, with P pathway focusing on the details and resolution and M pathway being more important in the nocturnal light. Between the laminae there is a spacing with koniocellular cells which share common features of the processing of both parvocellular and magnocellular laminae. [57]

From the LGN, visual information is then sent to the visual cortex in the occipital lobe. The visual cortex is composed by six layers with layer 4 being the one that receives the sensorial input, therefore being thicker, and layer 5 being the one that sends the output to other brain areas. Information from the P and M pathway can be processed in parallel in the cortex, in the spiny stellate neurons, or can converge in the pyramidal neurons.[57]

From here we can distinguish two different pathways based on their functionality: the dorsal pathway, located in the parietal lobe, and the ventral pathway, in the temporal lobe. The ventral pathway, also known as the stream for the "vision for perception", is responsible for the recognition and identification of an object, receiving a strong input from the P pathway, while the dorsal pathway, known as the "vision for action", is associated with the control of the movement, being responsible for both processing the spatial location and the movement of an object, therefore receiving a strong input from the M pathway. The dorsal stream has a much faster response than the ventral stream.[58] The primary visual areas V1, V2 and V3 are common to both pathways branching into two different streams after. The ventral pathway goes from the V3, or from V2, into the V4 and the Inferior Temporal cortex (IT) while the dorsal pathway goes from the V3, or from V1 or V2, to other dorsal regions such as the V5, also known as the Middle Temporal area (MT), and the Medial Superior Temporal area (MST). [58]

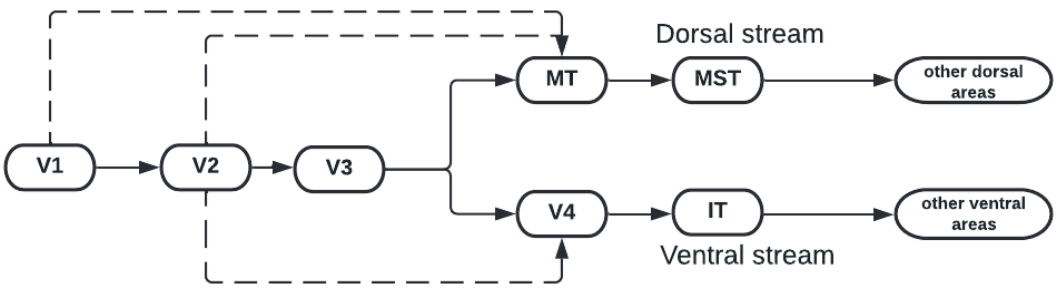

Figure 4. Schematic representation of the central visual pathways: the dorsal stream, the pathway for the 'vision for action' and the ventral stream, responsible for the 'vision for perception'.

The primary visual area V1 contains a map of the visual field covered by both eyes with the left V1 mapping the information from the right hemifield and the right V1 covering the information from the left hemifield. V1 receives the visual information and leads it to the secondary visual area V2 where it starts to be processed on a higher level regarding more detailed parts of what is being seen. It is then forwarded to the area V3 where the information from both eyes is further integrated. This process of integration is called binocular fusion. While area V4 is responsible for the processing of colour, MT is responsible for the processing of movement. [58]

The information that reaches MT can either be integrated, where the information from all the moving parts is compressed into one single object, or segregated, in which the information from the different moving parts is perceived as being from different objects. This decision which seems to be implemented in MT of either we are seeing a single object or various objects is called perceptual decision. This information is then led to other areas for a higher level processing. [58], [59]

One example can be when we perceive motion signals from a human being. The MT+ complex sends afferent signals to STS. While posterior STS is activated by coherent kinematic patterns, not being activated by scrambled motion [60], anterior STS shows greater response to moving faces. In communication with the STS is the Extrastriate Body area (EBA), which is situated inferior and posterior to the STS, which is activated in response to moving bodies. [58]

Recent studies have suggested the existence of a third pathway, that begins in the V1 and projects itself into the STS through the MT, which is not focused on the perception of an object but in the dynamics of the social perception. [58]

1.5. Biological Motion

The motion of living organisms, both people and animals, either the whole body or just parts, is designated as biological motion. The need for processing biological motion has always been a part of human life, either for survival purposes or in social interactions, and the capacity to process this information is developed so early as in infancy. [61] Therefore, not surprisingly, biological motion is thought to be an automatic, passive process, involving mostly low-level visual mechanisms. Nevertheless, the perception of biological motion is affected by attention and other top-down factors. [62]

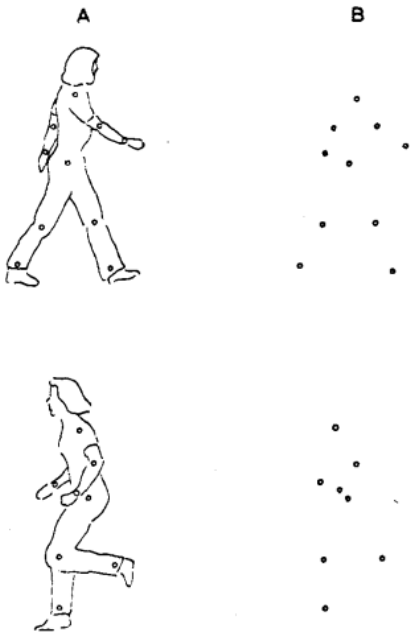

Figure 5. Example of the first point-light displays of human figures designed by Johansson in 1973. Representation of the human figure walking and running. Source: [63].

In 1973, Johansson discovered that biological motion could be accurately represented using point-light displays (PLD) (Figure 5). PLDs are displays of bright spots, usually 10 to 12 spots when representing human figures, that are located in the main joints of the body. Through the movement of these points that follow the patterns of the motion of the human or animal represented it is possible to recognize the action portrayed, such as walking, running, jumping or throwing an object, as well as to differentiate the gender, the emotional state and even recognize a friend or family members. [61], [63]–[66]

Figure 6. Snapshot taken from a video of a point-light walker. The data used in this thesis was motion captured data from a walking person from an online database. [67]

For example, walking can be represented as the group of smaller pendular movements from each joint of each part of the body. Representing the body through the major joints allows the creation of a stimulus stripped of any added information, therefore focusing only the attention on the motion patterns. PLDs representing human figures walking are often referred as point-light walkers (PLW).

The joints of the human body are ending points of each bone that are placed apart at a constant length. Therefore, they can be used as representative forms of the biological motion. The number of joints needed to perceive biological motion does not need to be very high. In fact, the visual system is very attuned to biological motion and is capable of distinguish motion in very degraded conditions and with very little information such as a total of 5 points of light to represent a human figure. However, the reaction time of the perception of biological motion decreases with the increase of the number of dots. [61]

There are two main methods to create this type of stimulus. The first method consists of motion capture from actors or non-actors who carry sensors in the joints which motion we pretend to capture. These videos are later processed to create a final video that will consist of the motion of the joints represented as either bright or dark spots against a contrasting background. The second method consists of the creation of artificial biological motion using algorithms that are based in data collected from the movements of several actors or non-actors.

The collected data can be manipulated through two forms: spatially, by changing positions and/or orientations of the points and/or adding or subtracting points; or temporally by changing the velocity of the points. It is known that the removal of certain points is detrimental for the perception of a PLD as a human figure. The most relevant points seem to be the ankle and the wrist points.[68]–[70]

Since the creation of PLDs to study biological motion, there have been a high number of studies in this area that allowed us to establish a network of brain areas related to the processing of biological motion (Figure 7). The processing of biological motion stimuli comprehends three major steps: firstly, the detection of the features of the stimulus and the subsequent coding of those features, followed by the integration of the features into a representation of a specific action, and finally, the decoding of the action and the agent based on prior knowledge. These mechanisms do not integrate the information linearly, rather seem to adapt to the nature of the stimuli. [61], [62]

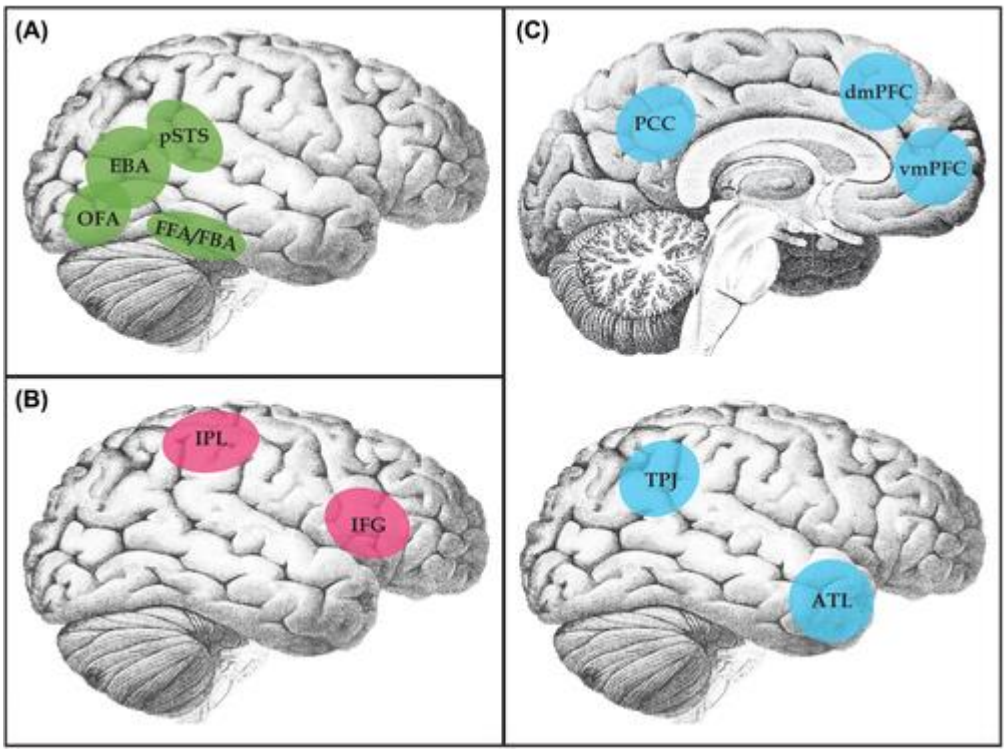

Figure 7. Brain areas activated while observing body expressions: occipital face area (OFA), extrastriate body area (EBA), posterior superior temporal sulcus (STS), fusiform body area (FBA), fusiform face area (FFA), dorsal medial prefrontal cortex (dmPFC), ventral medial prefrontal cortex (vmPFC), posterior cingulate cortex (PCC), inferior parietal lobule (IPL), inferior frontal gyrus (IFG), temporoparietal junction (TPJ), and, anterior temporal lobe (ATL). Source: [71].

Considering the main three steps of processing previously described, we can associate certain areas to each step. EBA and MT+ are responsible for the detection and decoding of the features of the stimulus. While MT+ detects motion and decides if it is biological motion or not, EBA, which is an area specifically for the processing of bodies, seems to be a more specific area for biological motion processing, presenting a higher level of activation when presented with the whole human body or parts of it. The Superior Temporal Sulcus (STS) also shows a higher level of activation for biological motion stimuli in comparison to other types of motion. This area is also responsible for the encoding of the actions processed by EBA and MT+ creating motion representations of these actions based on the patterns of the human articulations. [62] Biological motion perception is orientation specific: we can easily perceive a walking person through their representation as a PLD but when we invert the video, rotating it 90º, we can no longer visualize a person walking. The perception of the structure of the motion involves several brain areas such as the cerebellum, the intraparietal sulcus (IPS), the postcentral and the superior frontal gyrus, the Superior Parietal Lobe (SPL), and the MT+ complex.[72], [73]

The representations created in STS allow other brain areas to process the "agent" intentions behind the stimulus. Inferior Parietal Lobe (IPL), SPL and anterior intraparietal sulcus (aIPS) seem to be essentially goal-based oriented disregarding the effectors, not responding to the form and motion of the action. [62]

There are some other areas activated in the presence of these stimuli, such as ventral prefrontal cortex (vPMC) and IFG. Both of these areas show a higher level of activation for whole body stimuli and use an effector-based approach to assess the intention behind the action. It is thought that STS also has a role in understanding the intentions behind an action since STS seems to present a greater activation when faced with unexpected outcomes of an action. The medial prefrontal cortex and the temporoparietal junction (TPJ) have also been linked to the understanding of the intentions behind an action. [62], [74]

It is widely believed that the human brain is endowed with a mirror neuron system, which was originally demonstrated in monkeys, where neurons fire potentials for not merely the performance of the observed action but actually the observation of said movement by another agent without oneself creating the movement. [75]

The perception of biological motion requires the integration of information of both local and global cues. Therefore, we can divide the perception and processing in two different categories: biological form and biological kinematics. The perception of biological form seems to be based on the global form of the stimulus and it seems it is processed mostly in the dorsal stream while the biological kinematics is based on the information from the local cues processed in the ventral stream. Perturbing local motion trajectories by adding noise to PLDs but preserving the global form, for example, does not affect the perception of biological motion, suggesting these aspects are independent from each other. [76]

In fact, recent evidence has established a two-stage processing for biological motion, with the first stage focus on the processing of local cues in both dorsal areas such as MT+ complex and V3A, and ventral areas, like EBA and fusiform gyrus (FFG), while the second stage is supported majorly by the STS that functions as a hub, integrating information from both the first stage of processing as well as global information yet to be processed. STS is also connected to several other low-level regions that aid to the processing of motion, such as the cerebellum. [73]

Apart from the mentioned regions, Fusiform Body Area (FBA), IFG, Ventral Lateral Nucleus (VLN) are also linked to this process responding to both local and global cues.
The information of both global form and local cues are first processed in the cortical regions in the V1 to V3 areas and then continue in areas such as EBA, Fusiform Body Area (FBA), IFG, Ventral Lateral Nucleus (VLN) and STS. In these areas the information is discriminated between global form and local information. For the local information which gives us information on the biological kinematics, the information is also discriminated between natural and manipulated by some regions within the Default Mode Network (DMN), which comprises areas such as PCC, the medial prefrontal cortex (PFC), IPL and IFG. DMN regions show stronger connections to areas such as STS and Supplementary Motor Area (SMA) in the presence of human figures in comparison to abstract forms and when the movement of those follow natural motion patterns as opposed to non-natural motion patterns. [73], [77]–[79]
Although there is no a spatially distinction between the processing of local and global clues, there is a clear temporal distinction: on the first stage, there is the detection of local cues and resulting information of this stage is then fed into the second stage that consists of the integration of global information into the creation of a global shape. [73]

1.6. Emotion Perception in Biological Motion

Emotion perception is a highly complex process involving several brain areas involving the following processes: to perceive the emotions expressed from others, to regulate our own ones and to organize responses to those.

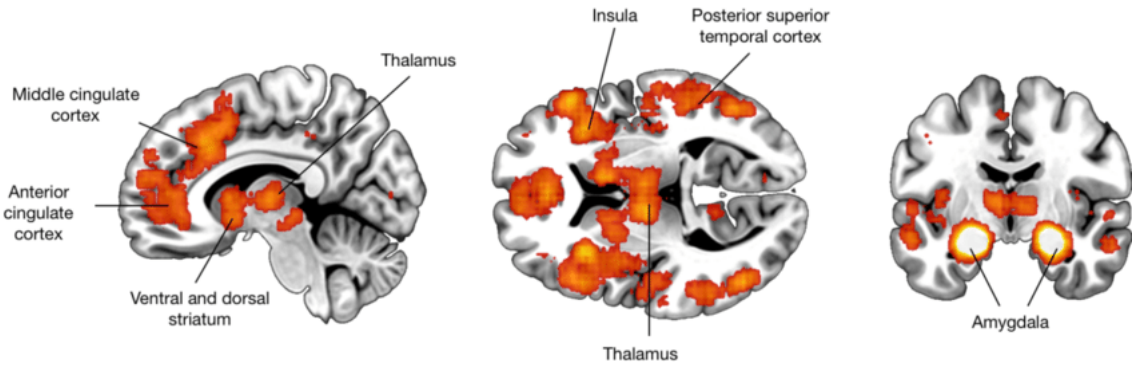

Figure 8. Brain areas involved in the emotion perception and processing. Source:[80]

The limbic system is located in the parietal and temporal regions of the brain and it is responsible for the control and regulation of emotions. It is constituted by three principal structures: the amygdala, which is responsible for the unconscious response to the emotions and for the regulation of both aggression and sexual behaviours; the hippocampus, that is responsible for the formation of memories and for the recognition and navigation of the surrounding space; and the hypothalamus, which controls the autonomous nervous system and, therefore, is responsible for the hormonal responses to the emotions as well as maintaining the homeostasis of the organism. In addition to these structures, there are also two other regions important to this system: the cingulate gyrus, which projects from the mammillary bodies, which are located in the hypothalamus, to the hippocampus; and the parahippocampal gyrus. [57], [81]–[83]

The prefrontal cortex (PFC) is associated with high level cognitive skills, such as the perception and integration of all the information that reaches the brain, either it is external, like the sensorial inputs, or internal, such as information regarding the homeostasis of the organism in order to plan responses and generate actions. PFC is divided in several areas with distinct functions such as the orbitofrontal cortex (OFC), which controls impulses and the regulation of the mood; the ventromedial prefrontal cortex (vmPFC), which is responsible for the conscious responses to emotions; and the insula.[57], [84], [85]

Both the brainstem and the cerebellum constitute the classically called reptilian brain, which is responsible for the instinctive behaviour and for the actions necessary for the survival, organizing unconscious responses to the surrounding environment and controlling the ‘fight or flight’ system. [57], [86]

These three systems are connected and communicate among them, planning complex responses to regulate the emotions and the survival instincts of the organism. This communication is regulated by excitatory and inhibitory neurotransmitters, as well as neuromodulators and neuropeptides. [57]

Biological motion comprehends information about both dynamics, such as motion direction and velocity, but social information, including information about gender, intention, social dominance and emotional states. PLD are a good way to study the perception of emotions in biological motion since it allows us to obtain a stimulus free of additional information, focusing only in the motion itself and what emotions it can

express. Emotional state perception can be influenced by the emotional state of the viewer, including their level of anxiety, their level of empathy and their inhibition capacity.[29], [46], [64], [65].

Several studies using facial expressions portraying different types of emotions as stimuli reported a possible preference of the brain for happier expressions, not only the performance in detecting happier expressions was better but there also seems to exist a faster switch to the perception of happiness, when we come from a negative emotion, and a slower switch to a more negative perception, when we start from a happier expression. [46], [50] This effect, named happiness superiority effect, is thought to be related with the fact that we are often more familiar with happier facial expressions and therefore are more trained on recognizing this emotion in social interactions. Adding this factor and the dependence of the emotions in biological motion processing on some brain areas common to the recognition of emotion in the facial expressions, it is not surprising that when exposed to stimuli of happy, sad and angry walkers, participants have a better score reporting happy walkers than compared to the angry and sad ones. [51]

Another heavy influence in experiments that deal with the emotion recognition is the mood of the observer. [52], [87] The phenomenon called emotional contagion, commonly known as empathy, describes the influence that our own emotional stage has on the perception of the emotional stage of the other. Emotional arousal influences attention, guides it to stimuli that are more likely to provoke an emotional response, such as signs of danger. For example, our discrimination skills improve after we are presented with a fearful face expression. The improvement of the discrimination skills is higher for fearful expressions when compared to neutral expressions, suggesting that extreme emotions can influence these attention mechanisms and consequently, the perception of the stimuli. [88] This effect on the attention mechanisms translates into an influence over the perception and could be explained based on the influence of the amygdala, the principal area involved in the processing of emotions, over the visual cortex. Literature reports frequently show that a positive emotion seems to benefit the global perception while negative emotions tend to increase the preference for a local perception.[89]–[92]

When combining biological motion and emotion there seems to be a distinct differentiation between the processing of images and videos of biological motion. While the static images seem to rise a higher activation in the FFA, the amygdala and the

temporal pole, the naturalistic videos provoke a higher activation on the EBA, Fusiform Body Area (FBA), FFA, TPJ and STS. [64], [93]

1.7. Methods for studying sensory perception

This project is structured in two main parts: a psychophysics study and functional Magnetic Resonance Imaging (fMRI) acquisition and analysis. While psychophysics enables the testing of the hypothesis and models underlying the perceptual mechanisms we are studying, fMRI allows for the understanding of the neural correlates responsible for the perceptual responses to the presented stimuli.

1.7.1. Psychophysics

Psychophysics aims to study the relationship between a presented stimulus and the sensory response provoked by it, by measuring the performance of the participant regarding previously determined factors. [94]

As the word itself suggests, psychophysics is the result of the interaction of psychology and physics with the objective to measure physical constraints of the human performance that results from a group of complex neural mechanisms. Furthermore, psychophysics provides a simple way to acquire quantitative measures of the responses and to study sensory processes as a first step to understand complex processes underlying the human responses to sensory input. This allows for linking psychophysical data with biological and imaging data and to draw conclusions based on that.[94]

Usually psychophysics studies aim to measure thresholds needed to evoke a certain perception of the stimulus, here we will instead measure transition points, that is, the point in which there is a change of perception from one emotion to another.

1.7.2. Functional Magnetic Resonance Imaging

Functional magnetic resonance imaging (fMRI) is a non-invasive imaging technique that uses changes in the blood oxygenation as a way to study brain activity. fMRI experiments are conducted with the objective of mapping patterns in the neuronal activation regarding a specific task performed by the subject. [95], [96]

The Magnetic Resonance Imaging (MRI) technique was created on the basis of the well-known physical properties of the protons that constitute the entire body. These protons are randomly oriented in a normal state but when placed in a strong magnetic field, such as the one created by the MRI scanner, the nuclei align in the field, creating a net longitudinal magnetization in the direction of the field. If this equilibrium is perturbed by a radiofrequency (RF) electromagnetic field pulse, the nuclei align along the direction of the pulse and get in phase, creating a transversal magnetization. Removing the RF pulse will cause the nuclei to go back to their original positions by emitting the energy they absorbed, generating a signal that is received by a receiver coil. This process is called longitudinal relaxation and it can be described by a time constant T_1. Simultaneously, there is a loss in the transverse magnetization as the nuclei de-phase in a process called transverse relaxation that can be described by a time constant T_2. [96], [97]

The type of tissue influences both T_1 and T_2values, which allows to the creation of structural MR images. T_2^* is similar to T_2 but with an added dependency on the local changes of the magnetic fields caused by the blood flow and the oxygenation, thus allowing to obtain functional MR images taking advantage of the blood oxygenation level-dependent (BOLD) effect. [96], [97]

The BOLD effect describes an increase of blood flow in the neuronal areas activated by a task to answer the higher demands of both nutrients and oxygen in these regions. This creates changes on the ratio of oxygenated and deoxygenated hemoglobin present in the blood which have pretty distinct different magnetic properties: the relaxation rate of oxygenated hemoglobin is longer than the relaxation rate of the deoxygenated hemoglobin which generates different signals in the tissues according to their activation levels. This change in the MRI signal is often referred to as the hemodynamic response function (HRF) and follows a very characteristic pattern. [96], [97]

The data acquired in fMRI experiments consist of temporal sequences of 3 dimensional MRIs, constituted by uniformly spaced voxels with a specified size. The total number of brain volumes acquired depends on the duration of the task and the repetition time (TR) defined, which is the time it takes to acquire a whole 3D volume of the brain. [95], [98]

Chapter 2. Behavioural Experiment

2.1. Methods

2.1.1. Creation of the stimuli

For the creation of the stimuli, it was used *MATLAB R2020b*, the *Psychophysics Toolbox Version 3* (http://psychtoolbox.org/) and the *BiomotionToolbox*. [99], [100]

We used motion captured data from real people which were then manipulated instead of creating motion patterns based on algorithms. Using real data allows for a more natural approach of the situation, making the motion patterns to look as real as possible.

The data used for the creation of the stimuli used in these experiments were taken from the online open access library of motion captured data for the study of problems of identity, gender, and emotion perception from biological motion.[67]

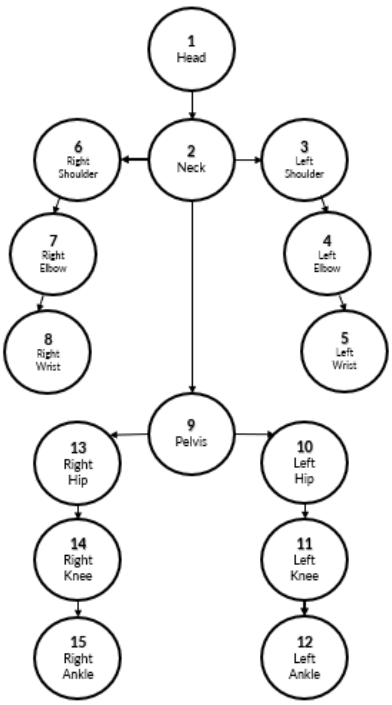

Figure 9. Representation of a point-light walker and correspondence to the human articulations created with the information provided by the database.[67]

This database comprises several files of different actions, including walking, combined with different emotions, including sadness, happiness, anger and in a neutral state, for each of the actors. The actions were performed by nonprofessional actors to avoid over exaggerated actions and to obtain a wider variety of expressions of the emotions. The actors were given a script with a scenario and the intended emotion and were given a fifteen-minute training the day before the recording of the actions. For this project, only the walking data combined with the neutral expression and two emotional states, happy and sad, were used. [67]

The best three actors were selected from the available data regarding the expression of the desired emotions, one female actress and two male actors, with ages comprehended between twenty-one and twenty-five years old.

First, we selected the frames that comprise a single step for each of the three states. Using a linear interpolation to recreate the missing frames between the last frame of the step and the first frame of the step, we obtained a fluid transition between each step resulting in a cycle of 21 steps in which the morphing level between the first emotional and the neutral stage followed by the morphing of the neutral and the second emotional stage was increased at a certain temporal step.

Figure 10. Sequence of snapshots from one of the dynamic transitions created.

For the morphing of the emotion into the neutral stage, we created a trajectory in which each step represented a different level of morphing starting with 100% of the first emotional stage, happy or sad depending on the direction, and decreasing the weight by 10% of the first emotion while simultaneously increasing the weight of the neutral stage by 10% until the neutral represented 100% of the weight of each joint. The same process

was applied from the neutral stage until the other extreme of the transition, the other emotion. Each full step that corresponded to a cycle of morphing used up 90 frames which resulted in a duration of 0.9 seconds per step.

To avoid the overlapping of the change of percentage of emotion and the start of another step, the first and last step were 100% of the emotion at the extreme and the change of emotion started at the 40th frame of the following step. Therefore, the duration for this percentage was slightly longer than for the rest of the percentages (Table 3).

Table 3. Frame intervals correspondent to each percentage of emotion according to the design of the stimulus to be presented at a frame rate of 100 Hz.

First frame	Last frame	Emotion 1	Neutral	Emotion 2
1	138	100	0	0
139	236	90	10	0
237	334	80	20	0
335	432	70	30	0
433	530	60	40	0
531	628	50	50	0
629	726	40	60	0
727	824	30	70	0
825	922	20	80	0
923	1020	10	90	0
1021	1118	0	100	0
1119	1216	0	90	10
1217	1314	0	80	20
1315	1412	0	70	30
1413	1510	0	60	40
1511	1608	0	50	50
1609	1706	0	40	60
1707	1804	0	30	70
1805	1902	0	20	80
1903	2000	0	10	90
2001	2148	0	0	100

For the control conditions, we used snapshots of a step from the morphing stimuli using a step size of 20%. These snapshots were then presented in a randomized order.

2.1.2. Experimental Design

The behavioural experiment consisted of a total of 3 runs of dynamic transitions and 3 runs of the control conditions.

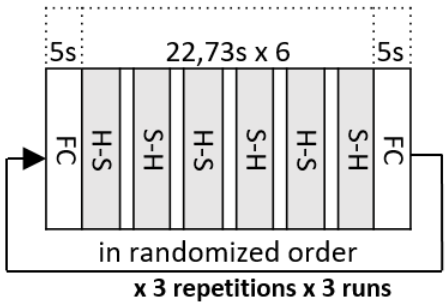

Figure 11. Example of the organization of a dynamic run with a total duration of 9.50 minutes consisting of 3 blocks with 6 trials each. Participants performed 3 of these runs.

In the dynamic transition, the PLW consisted of the 15 major joints of the human body (head, neck, left and right shoulders, left and right elbows, left and right wrists, pelvis, left and right hips, left and right knees, left and right ankles). Each run of dynamic transitions consisted of 3 blocks of 6 trials each. Each stimulus had the duration of 21.48 seconds followed by a black screen between each trial for 1.25 seconds to allow the participant to rest before the next trial which resulted in a total of 22.73 seconds per trial. At the beginning of each run as well as at the end of each block and the end of the run it was presented a fixation cross for 10 seconds. In total each of these runs had the duration of 9.50 minutes. Participants were instructed to indicate the perceived emotion via button press (see details below).

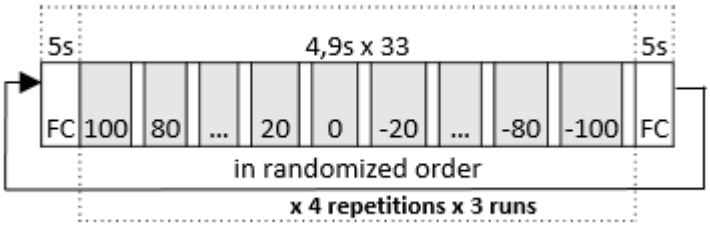

Figure 12. Example of the organization of a control run, with a total duration of 11,11 minutes consisting of 4 blocks with 33 trials each. Participants performed 3 of these runs.

For the control conditions, the stimulus consisted of a random snapshot of a single step with a certain percentage of one of the emotions. This run consisted of 4 blocks of 33 trials. Each stimulus had the duration of 0.9 seconds followed by a black screen for 4

seconds, resulting in a total duration of 4.9 seconds per trial and 161.7 seconds per block. At the beginning of each run as well as at the end of each block and run there was presented a fixation cross for 5 seconds. In total, each of these runs had the duration of 11.11 minutes.

During the control trials the participants were instructed to identify the emotion presented by pressing one of the three given buttons accordingly, either happy, neutral or sad. The control stimuli presented loose steps with different percentages of each emotion and with no sequential logic therefore eliminating any previous experience, history, allowing these data to be used as a control for the perceptual history effects.

2.1.3. Experimental Setup

In the behavioural experiment, the stimuli were presented using *MATLAB R2021b* and the *Psychophysics Toolbox Version 3,* in the centre of a liquid-crystal display (LCD) monitor with a resolution of 1440 x 1080 pixels, a refresh rate of 100 Hz and a luminance of 18.7 cd/m^2 in the black screen and of 150.2 cd/m^2 in the white screen. Participants were positioned at a distance of about 70 cm from the display screen.

We used Eyelink from SR-Research as an eye tracker system to record the movements and position of the eye and the pupil size for further research.

For both the dynamic transitions and the control conditions, the keyboard keys were previously chosen to correspond to each of the emotional states being the left arrow for sadness, the down arrow for neutral and the right arrow for happiness.

In the dynamic transitions, the participants were asked to press the keyboard key corresponding to the emotional state they first perceive at the beginning of each trial and then to press the key corresponding to the neutral stage when/if they perceived a change and again when/if they observed another emotional stage. For the control conditions, the participants were asked to press the button of the emotional state they perceived after the presentation of each stimulus.

2.1.4. Instructions

The instructions given to the participants were the following:

"You will participate in an experiment where you see images of walking bodies made of dots. You will have to judge whether they are happy or sad. This happens in two ways: short videos and long videos.

We will start each run by calibrating the eye tracker. For this part and throughout the experiment you should remain with your chin placed on the stand and as immobile as possible. For the calibration of the eye tracker, there will be a small white dot presented on the screen. You should follow it with your eyes. We will repeat this process two times and then start the experiment.

There are 3 keys on the keyboard that represent the 3 emotional states: the left arrow is for the 'sad' emotion, the down arrow is for the 'neutral' stage and the right arrow is for the 'happy' emotion.

In the long videos, when the video starts you must obligatorily report the first emotion you see (even if ambiguous) by pressing the keyboard accordingly with the emotion you perceive, happy or sad, and then report when/if it changes to neutral and/or when it changes to the opposite emotion.

In the short videos, you will see a single step presented followed by a black screen. You should observe the video first and then report during the black screen by pressing the key corresponding to the emotional stage you perceived: sad, neutral, or happy.

Please note that these videos were made with actors really expressing these emotions. Therefore, even if it looks ambiguous you always have to decide the first emotion. It may sometimes happen that there is not switch to neutral or the other emotion.

If you need to stop the experiment for any reason, you can press the 'esc' key. This will immediately end the video you are seeing."

2.1.5. Participants

Twenty-two healthy participants were recruited to participate in the behavioural experiment (13 females; mean age, 24,09±2,93 years). All had a normal or corrected-to-normal vision and no known history of neurological or psychiatric diseases. All participants were right-handed except for one, as confirmed by a handedness questionnaire adapted from [101] and available in https://www.brainmapping.org/shared/Edinburgh.php. Participants provided written informed consent prior to the experiment following protocols approved by the Ethics Committee of the Faculty of Medicine of the University of Coimbra, in accordance with the Declaration of Helsinki.

Table 4. Information of the volunteers that participated in the behavioural experiment.

ID	Age	Gender	Dominant Hand	Dominant eye	Laterality
01	24	F	R	R	R
02	22	F	R	R	R
03	31	F	R	R	R
04	29	F	R	R	R
05	22	M	R	R	R
06	22	F	R	R	R
07	26	F	R	R	R
08	29	M	R	R	R
09	26	F	R	R	R
10	21	F	R	R	R
11	28	M	R	R	R
12	22	F	L	R	L
13	26	F	R	L	R
14	21	M	R	R	R
15	22	M	R	L	R
16	22	M	R	L	R
17	30	F	R	R	R
18	21	M	R	L	R
19	21	F	R	L	R
20	21	M	R	R	R
21	22	M	R	R	R
22	22	F	R	R	R

2.2. Results

2.2.1. Group level analysis

2.2.1.1. Pre-analysis data treatment

The first step of the analysis was to divide and classify every trial, according to the responses given during the experiment, into one of four possible classifications:

- *completed trajectories*, E1-N-E2, where the three emotional states were identified by the participant in the correct order;
- *trajectories with instantaneous neutral state*, E1-E2, where the participant identified both the initial and ending emotions correctly but did not identify a transition to the neutral state between the two emotions;
- *trajectories persistent in neutrality*, E1-N, where the participant identified the first emotion correctly and a transition into the neutral state but persisted in the neutral state never transitioning to the other emotion;
- *invalid trajectories*, where the participant either identified the order of the emotions incorrectly or just identified one emotion or the neutral state.

The classifications of the trajectories according to these categories are presented in Table 5.

Only the trials classified as completed trajectories were used in subsequent analyses as these were the only trajectories including perceptual switches and that started and ended in the emotions intended.

Based on the design of the stimulus, the groups of frames were parametrized in terms of the percentage of positive emotion, being -100% sadness, 0% neutral and 100% happiness.

Using the number of the frames in which the participant reported the changes of perception and the correspondence of the groups of frames to the parametrization of the percentage of emotions, we attributed a percentage of emotion to each report. These percentages in the trajectories were then compared to the switch in the control curves.

Table 5. Number of trajectories of each class for each participant, according to the responses of each participant for the dynamic runs based on the defined criteria, with E1-N-E2 representing the completed trajectories; E1-N being the trajectories persistent in neutrality; E1-E2 representing the trajectories with instantaneous neutral state; and Invalid referring to the invalid trajectories.

		Actor 1				Actor 2				Actor 3			
Subject	**Direction**	E1-N-E2	E1-N	E1-E2	Invalid	E1-N-E2	E1-N	E1-E2	Invalid	E1-N-E2	E1-N	E1-E2	Invalid
01	Happy to Sad	1	7	0	1	9	0	0	0	8	1	0	0
	Sad to Happy	1	4	0	4	9	0	0	0	9	0	0	0
02	Happy to Sad	1	6	0	2	9	0	0	0	9	0	0	0
	Sad to Happy	1	6	0	2	9	0	0	0	8	1	0	0
03	Happy to Sad	2	3	1	3	2	0	7	0	8	0	1	0
	Sad to Happy	0	0	2	7	7	2	0	0	8	1	0	0
04	Happy to Sad	5	1	1	2	4	0	1	4	9	0	0	0
	Sad to Happy	1	2	0	6	8	1	0	0	8	1	0	0
05	Happy to Sad	1	3	0	5	2	0	1	6	8	1	0	0
	Sad to Happy	2	1	0	6	4	5	0	0	8	0	1	0
06	Happy to Sad	1	3	0	5	6	1	0	2	9	0	0	0
	Sad to Happy	2	6	0	1	7	2	0	0	9	0	0	0
07	Happy to Sad	7	1	1	0	8	0	0	1	9	0	0	0
	Sad to Happy	5	0	0	4	9	0	0	0	8	0	1	0
08	Happy to Sad	6	0	0	3	9	0	0	0	9	0	0	0
	Sad to Happy	6	3	0	0	9	0	0	0	8	0	1	0
09	Happy to Sad	3	4	0	2	7	0	0	2	9	0	0	0
	Sad to Happy	6	1	0	2	9	0	0	0	9	0	0	0
10	Happy to Sad	2	4	0	3	6	3	0	0	6	3	0	0
	Sad to Happy	4	0	0	5	5	1	0	3	6	0	0	3
11	Happy to Sad	8	0	0	1	9	0	0	0	9	0	0	0
	Sad to Happy	8	0	0	1	9	0	0	0	8	1	0	0
12	Happy to Sad	1	8	0	0	9	0	0	0	8	1	0	0
	Sad to Happy	6	2	0	1	7	2	0	0	8	1	0	0
13	Happy to Sad	2	6	0	1	9	0	0	0	9	0	0	0
	Sad to Happy	8	0	0	1	9	0	0	0	9	0	0	0
14	Happy to Sad	1	5	1	2	7	0	2	0	7	0	1	1
	Sad to Happy	1	5	1	2	7	2	0	0	7	2	0	0
15	Happy to Sad	8	0	0	1	7	1	0	1	9	0	0	0
	Sad to Happy	4	1	0	4	9	0	0	0	9	0	0	0
16	Happy to Sad	7	0	0	2	8	0	0	1	9	0	0	0
	Sad to Happy	5	0	0	4	9	0	0	0	9	0	0	0
17	Happy to Sad	0	2	0	7	2	0	2	5	6	2	1	0
	Sad to Happy	0	1	0	8	5	4	0	0	7	1	1	0
18	Happy to Sad	6	2	1	0	8	0	1	0	8	0	0	1
	Sad to Happy	7	1	0	1	7	2	0	0	6	3	0	0
19	Happy to Sad	0	3	0	6	8	0	0	1	9	0	0	0
	Sad to Happy	2	0	0	7	8	1	0	0	9	0	0	0
20	Happy to Sad	2	7	0	0	9	0	0	0	8	0	1	0
	Sad to Happy	2	2	0	5	6	3	0	0	7	1	1	0
21	Happy to Sad	5	2	0	2	8	0	0	1	9	0	0	0
	Sad to Happy	8	0	0	1	9	0	0	0	9	0	0	0
22	Happy to Sad	8	1	0	0	9	0	0	0	9	0	0	0
	Sad to Happy	7	1	0	1	7	2	0	0	9	0	0	0

2.2.1.2. Control Curves

To obtain the control curves, we calculated the percentage of neutral reports (the total number of neutral reports divided by the total number of answers) for each percentage of emotion displayed in the control stimuli. Since the stimuli was created based on the motion data captured from three different actors, we traced the control curves for the three actors separately to assess possible differences perceived by the participants.

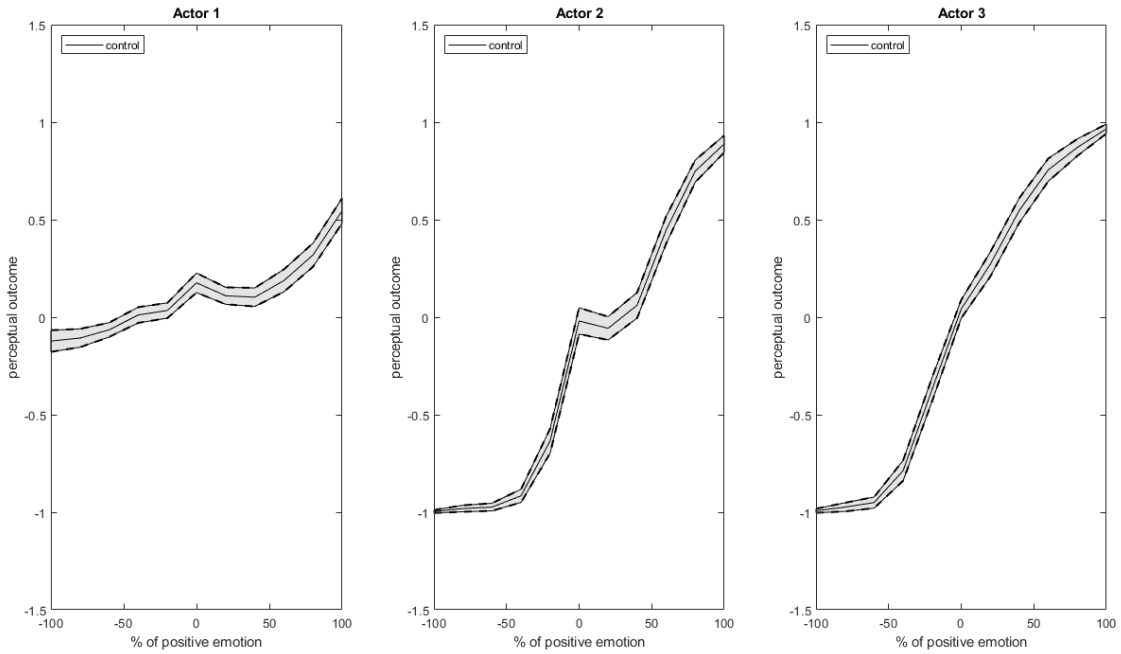

Figure 13. Graphs of the control curves of the group obtained for each actor using the data collected in the control runs that consisted of the attribution of one of the 3 emotions to each of the presented snapshots. The shaded area represents the confidence interval of 95%. In the y-axis, is represented the perceptual outcome with 1 being happiness, 0 the neutral state and -1 sadness. The x-axis is parametrized according to the positivity of the emotion present on the videos, being -100% sadness and 100% happiness.

Comparing the three curves for each actor (see Figure 13), it is clear that there is a different level of ambiguity for each actor with the biological motion patterns from actor 1 being more ambiguous than the other two. A higher degree of ambiguity in the perception of the emotion of an actor translated itself into a close to linear control curve instead of the expected sigmoid. This ambiguity can be explained by several different factors such as the fact we are using real motion captured data performed by amateur

actors which might lead to not so clear representations of the reality, and the actors themselves might have different levels of expression regarding these emotions as each human being is unique in expressing their emotions. Furthermore, perceiving and expressing the emotions through the motion might be more difficult than for facial expressions.

This conclusion led to another question: if the control curves did not all present a sigmoid form, did the perception of the emotions follow a linear pattern, passing through the three emotional states at the same rate or did they follow a sigmoidal pattern, spending more time in the extreme emotions, sadness and happiness, and going through the neutral state in a faster motion?

To answer this question, we plotted the data points of the mean of the responses for each emotional percentage, as exemplified in Figure 14, and applied both the linear regression and the sigmoidal function and calculated the R^2 for both the regressions.

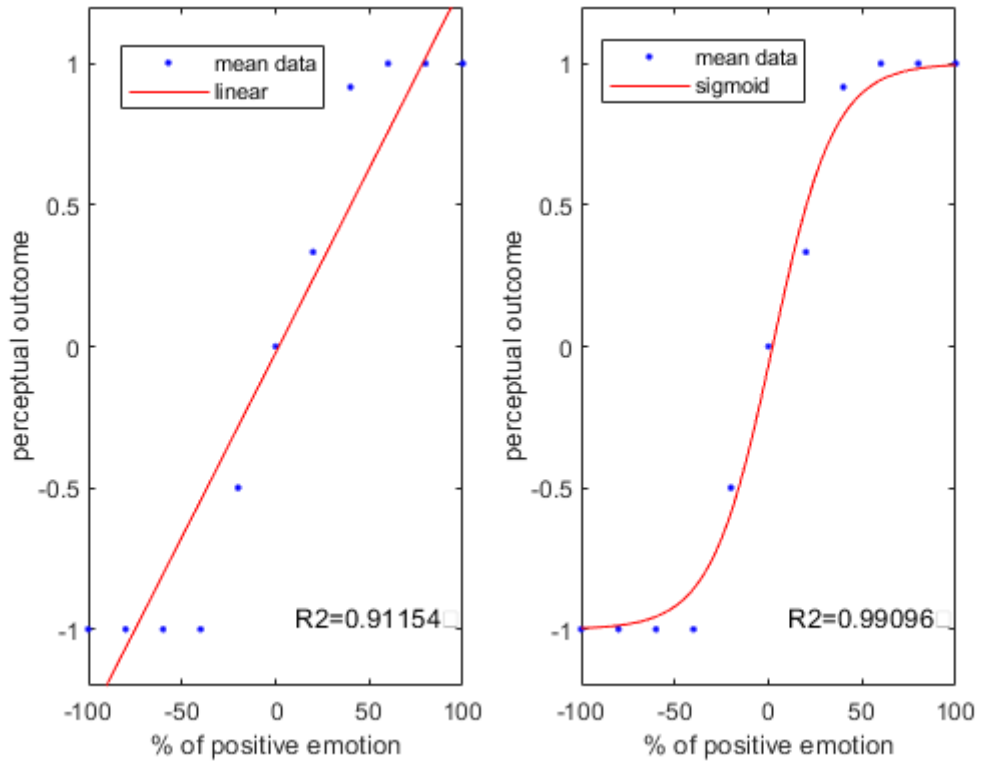

Figure 14. Example of the regressions of a control curve using a linear regression on the left, and a sigmoidal regression on the right. The data used for these graphs corresponds to the data collected in the three control runs of one participant for actor 3. Sigmoidal regression presents a better adjustment as visually observed and confirmed by the value of the R^2.

Table 6. R^2 values for the linear and sigmoidal regressions obtained for the control curve of each actor for each participant.

Subject	Actor 1		Actor 2		Actor 3	
	Linear	Sigmoidal	Linear	Sigmoidal	Linear	Sigmoidal
01	0.32671	0.32588	0.90661	0.92445	0.93798	0.98092
02	0.56640	0.55378	0.89450	0.91153	0.92855	0.98289
03	0.87302	0.86477	0.92103	0.96809	0.94338	0.98899
04	0.59645	0.59111	0.91158	0.89303	0.95080	0.97329
05	0.27110	0.27007	0.90513	0.87844	0.96040	0.96851
06	0.26379	0.26388	0.90964	0.87623	0.98610	0.97547
07	0.68776	0.67640	0.82751	0.94835	0.86953	0.99793
08	0.73606	0.71376	0.92192	0.96859	0.89039	0.89057
09	0.69818	0.69312	0.95863	0.95680	0.96426	0.98092
10	0.74462	0.74343	0.87165	0.97071	0.94495	0.96728
11	0.53018	0.52338	0.93357	0.96944	0.91154	0.99096
12	0.66777	0.62767	0.92164	0.95448	0.90704	0.98570
13	0.76587	0.72776	0.91490	0.93127	0.93998	0.96615
14	0.83913	0.81120	0.95291	0.98593	0.93167	0.97311
15	0.58824	0.58340	0.91180	0.94060	0.91177	0.99361
16	0.78835	0.77621	0.90211	0.91242	0.94586	0.99266
17	0.77668	0.75742	0.87520	0.84357	0.96837	0.96833
18	0.80437	0.81002	0.82227	0.94604	0.90845	0.90779
19	0.42093	0.41823	0.89742	0.96922	0.93107	0.95042
20	0.74074	0.73771	0.88815	0.92383	0.96231	0.98166
21	0.24691	0.24594	0.91460	0.94690	0.93814	0.96636
22	0.42875	0.42311	0.84142	0.85308	0.96213	0.98742

Comparing the data for both actors 2 and 3, in general, for all the participants, the best function adjustment to the control data was the sigmoidal regression which presented a higher value for R^2 (see Table 6). For actor 1, the values for R^2 show a deviation from this pattern, which is not unexpected given the large level of ambiguity.

In conclusion, normal emotion perception under control conditions (absence of history) presents a non-linear (sigmoidal) behaviour with the emotions, sadness and happiness, overruling the perception of the neutral state until reaching the point of transition, which is estimated to be different from participant to participant (Table 7 – Actor 1 was excluded from this analysis given the large perceptual ambiguity at all points, and the difficulty in estimating the transition point). The neutral perception is briefly hold before the change to the other perception.

Table 7. Percentages of emotion at the point of neutral state perception for actor 2 and actor 3 for each participant.

Subject	positivity of emotion at the neutral point	
	Actor 2	Actor 3
01	30	0
02	10	-10
03	0	0
04	20	10
05	30	0
06	40	0
07	-10	-10
08	0	-10
09	40	0
10	50	0
11	10	0
12	-10	-10
13	40	0
14	20	20
15	40	0
16	40	10
17	-10	-10
18	50	40
19	30	0
20	50	0
21	40	0
22	40	10

The neutral point is the point where the control curve crosses with y = 0, being the y-axis the perceptual outcome, with -1 being sadness, 0 the neutral state and 1 happiness. Theoretically, this point should be located at x = 0, being the x-axis the axis of the positivity of the emotion and 0 the point where the videos presented are exactly the same as the original videos where the actors acted as being in a neutral state. As previously stated, emotion perception is an individual-specific process affected by a number of

factors that makes it unique for each of us and therefore, even watching the exact same videos, the neutral point changes across participants.

It should also be mentioned that for actor 2 the neutral point varies from -10 to 50 % of positivity while for actor 3 it varies from -10 to 40 % with several participants with a neutral point equal to x = 0 or closer to it than in actor 2. This suggests that actor 3 shows more cases with less bias than actor 2, but only a slightly lower variance, which is in accordance with the curves previously traced and the R^2 values obtain for the sigmoidal regressions of the control curves.

2.2.1.3. Dynamic transitions

Using the data from the trajectories where the subjects correctly identified the trajectory and the three emotions, the mean trajectory for each direction and each subject was traced and then the mean of those to achieve the mean trajectory of the group for each direction. This was calculated separately for three actors given the differences found while studying the control curves. The results are presented in Figure 15.

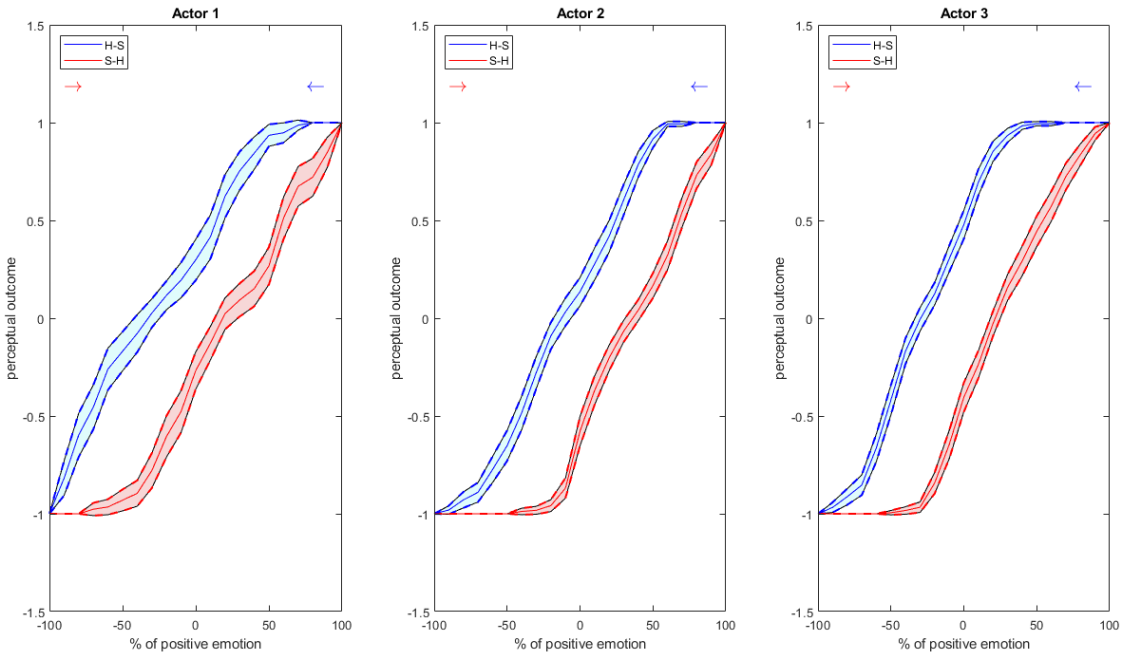

Figure 15. Group averages of each direction for each actor for the dynamic transitions separated by the two directions. In blue is represented the direction 'happy to sad' and in red is the direction 'sad to happy'. The shaded areas represent the confidence interval of 95%. In the y-axis, is represented the perceptual outcome with 1 being happiness, 0 the neutral state and -1 sadness. The x-axis is parametrized according to the positivity of the emotion present on the videos, being -100% sadness and 100% happiness.

For all the three actors, there is a clear spacing between the trajectories of both directions suggesting they are entirely independent from each other. Therefore, we can state that there is a clear effect of the history on the perception of the current stimulus as the path of perception from happy to sad is not the same as the path from sad to happy, which confirms the existence of perceptual hysteresis.

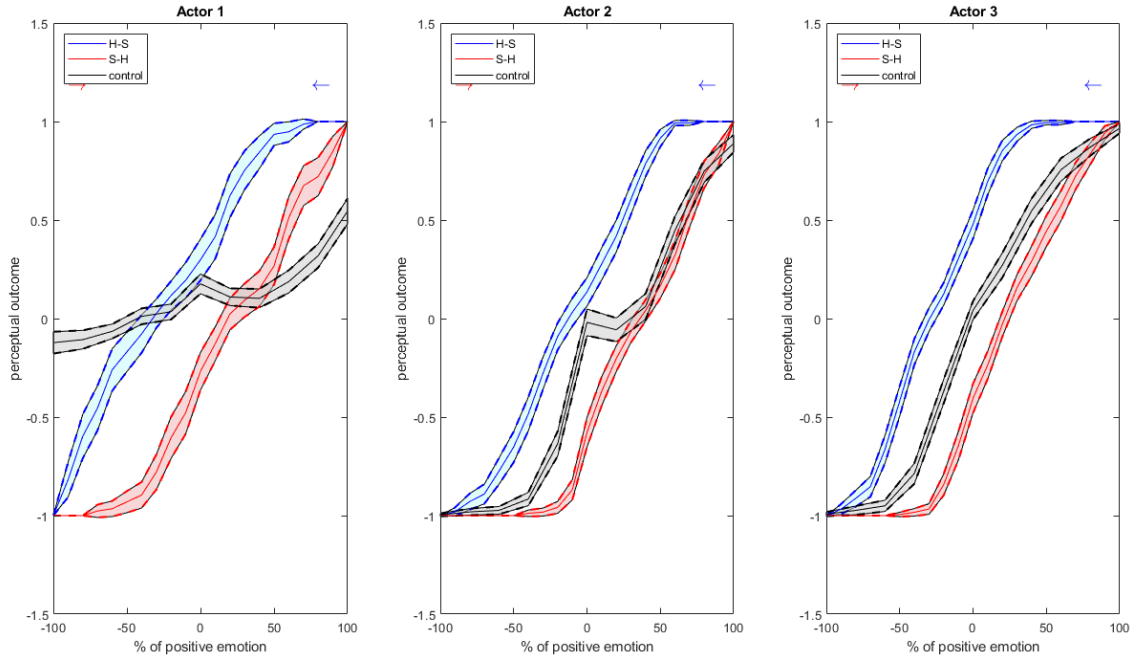

Figure 16. Group averages of each direction, with red being the direction 'sad to happy' and blue the direction 'happy to sad', and the control curve, in grey, for each actor. The shaded areas represent the confidence interval of 95%. In the y-axis, is represented the perceptual outcome with 1 being happiness, 0 the neutral state and -1 sadness. The x-axis is parametrized according to the positivity of the emotion present on the videos, being -100% sadness and 100% happiness.

Adding the control curves previously created to these graphs gives us a reference to the trajectory without the added effect of hysteresis, which gives us the possibility to classify the type of hysteresis of the group for actor 2 and 3 (Figure 16).

As previously stated, actor 1 presents an abnormal control curve which does not allow for the classification of the type of hysteresis in either of the directions. For this reason, actor 1 was excluded from the analysis of the results related to the type of hysteresis.

However, not being able to classify the type of hysteresis does not mean we cannot acknowledge the existence of it, as it is clear from Figure 15 that both directions follow different and well separated paths showing a clear effect of the history on the trajectory.

2.2.1.4. Inferential Statistical Analysis

To better analyse the existence of perceptual hysteresis, we proceeded to study the moment of the perceptual switch from the first emotion to the neutral state as well as the area between the curves of each direction and the control and between both directions, as these two factors are often mentioned in literature as measures of the hysteresis effect.

The first step in the statistical analysis was to study the data we obtained from the trajectories by testing its normality using the Shapiro-Wilk test.

Table 8. Results from the Shapiro-Wilk test performed to test for normality of the distribution of values of the perceptual switch moments for both directions and the control.

		Statistic	df	Sig.
Actor 1	Happy to Sad	0,952	20	0,393
	Sad to Happy	0,937	20	0,212
	Control	-	-	-
Actor 2	Happy to Sad	0,933	22	0,142
	Sad to Happy	0,953	22	0,361
	Control	0,877	22	0,010
Actor 3	Happy to Sad	0,929	22	0,119
	Sad to Happy	0,880	22	0,012
	Control	0,755	22	< 0,001

Table 9.Results from the Shapiro-Wilk test performed to test for normality of the distribution of values of the areas for both directions and the control.

		Statistic	df	Sig.
Actor 1	Happy to Sad	0,513	20	< 0,001
	Sad to Happy	0,702	20	< 0,001
	Control	-	-	-
Actor 2	Happy to Sad	0,707	22	< 0,001
	Sad to Happy	0,675	22	< 0,001
	Control	0,627	22	< 0,001
Actor 3	Happy to Sad	0,575	22	< 0,001
	Sad to Happy	0,706	22	< 0,001
	Control	0,490	22	< 0,001

The results from the Shapiro-Wilk test performed suggest that the distributions of the moment corresponding to the switch follow a normal distribution, presenting p-values higher than 0.05, with the exception of the direction sad-happy for actor 3 and the control for both actors 2 and 3 (Table 8). The distributions of the areas for both directions for the three actors as well as the controls for actors 2 and 3 present $p<0.001$, therefore not

following normal distributions. Given these results we performed non-parametric Wilcoxon signed-rank tests to assess for statistically significant differences between the two directions as well as each direction and the control (Table 9).

Table 10. Wilcoxon signed-rank test results for the perceptual switch moments for each direction and control and for both directions, separated by actor.

		Z	Asymp. Sig. (2-tailed)
Actor 1	Happy to Sad - Sad to Happy	-3,924	< 0,001
	Happy to Sad - Control	-	-
	Sad to Happy - Control	-	-
Actor 2	Happy to Sad - Sad to Happy	-4,060	< 0,001
	Happy to Sad - Control	-3,817	< 0,001
	Sad to Happy - Control	-2,159	0,031
Actor 3	Happy to Sad - Sad to Happy	-4,118	< 0,001
	Happy to Sad - Control	-4,127	< 0,001
	Sad to Happy - Control	-3,545	< 0,001

A Wilcoxon signed-rank test showed significant differences in the perceptual switch moment between each direction and the control for both actors 2 and 3 suggesting that the history does affect the perception of the presented stimuli (Table 10).

Comparing the perceptual switch moment of the three actors for both directions, 'happy to sad' and 'sad to happy', the Wilcoxon signed-rank revealed significant differences as well.

The same test was then performed using the distribution of the areas for each direction and the control, for both actor 2 and actor 3, but the results were not uniform for these comparisons, possibly due to the lower statistical power (Table 11).

Table 11. Wilcoxon signed-rank test results for the areas for each direction and control and for both directions, separated by actor.

		Z	Asymp. Sig. (2-tailed)
Actor 1	Happy to Sad - Sad to Happy	-2,940	0,003
	Happy to Sad - Control	-	-
	Sad to Happy - Control	-	-
Actor 2	Happy to Sad - Sad to Happy	-1,088	0,277
	Happy to Sad - Control	-1,477	0,140
	Sad to Happy - Control	-0,956	0,339
Actor 3	Happy to Sad - Sad to Happy	-2,029	0,042
	Happy to Sad - Control	-2,207	0,027
	Sad to Happy - Control	-0,886	0,375

While the Wilcoxon signed-rank test failed to show significant differences between each direction and the control for actor 2, it detected signficant differences for the direction ‘happy to sad’ and the control of actor 3 but not for the pair ‘sad to happy’ and control. When comparing both directions for actor 1 and 3, Wilcoxon signed-rank test showed significant differences but not for actor 2.

These results are unexpected given the graphical representation of both directions for each actor, and might be explained by underlying heterogeneity and reduced statistical power of non-parametric analyses. There is a clear spacing between both curves. However, the graphics only present the average for the means of all the subjects and by the results of the statistical analysis, we can conclude that the data is probably not homogeneous, with some subjects presenting stronger positive hysteresis than others. Furthermore, if there are cases of negative hysteresis in low number, this effect can be absorbed in the general mean but can possibly explain the results in the statistical analysis.

This led to the need to further explore the data collected by looking in detail to the trials used in this first analysis.

2.2.2. Subject level analysis

2.2.2.1. Defining hysteresis metrics

Classically we can measure hysteresis using two different metrics: the spacing between the curves of each trajectory or the distance of the two inflection points (corresponding to the change of perception from each emotion to the neutral state).

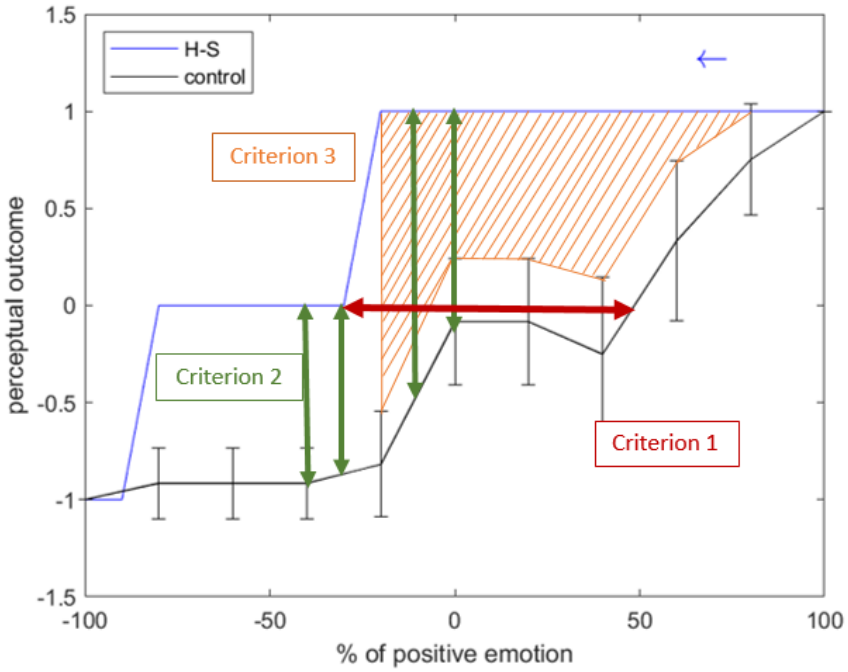

Figure 17. Example of a trajectory and the visual representation of the three criteria defined for the classification of the trajectories regarding the presence of hysteresis and the type of hysteresis. In the y-axis, -1 represents sadness, 0 the neutral state and 1 happiness, while in the x-axis, -100% is sadness, 0 neutral and 100% happiness.

Using both these metrics, we establish three criteria for the existence of hysteresis:

- **Criterion 1:** The distance of the x values of the trajectory and the control curve of the correspondent actor in y = 0 is different from zero.
- **Criterion 2:** The distance in y of the trajectory and the control curve of the actor for the two previous points and the two next points of the x value in which y = 0 is different from zero and is always positive or always negative, meaning the two trajectories do not cross during this period.
- **Criterion 3:** Considering the trajectory only until the x value for which y = 0, the area between the trajectory and the curve drawn using the confidence interval of the points of the control curve has to be bigger than the area between this curve and the control curve.

Using these criteria, we first classified each of the completed trajectories in two categories: trajectories with hysteresis and null trajectories (N). For a trajectory to be considered a trajectory with hysteresis it needed to fulfil at least two of the three criteria. The trajectories with hysteresis were then classified for the type of hysteresis.

We can distinguish hysteresis in two types: positive hysteresis (PH), or persistence, in which the participant holds the current perception for longer, causing a positive lag; and

negative hysteresis (NH), based on an adaptation mechanism, in which there is an early perceptual switch, causing a negative lag. We also considered a third category, undefined (UN), to encompass the trajectories where the behaviour of the curve initially seems to follow a pattern of hysteresis but it suddenly changes and starts to follow the control curve.

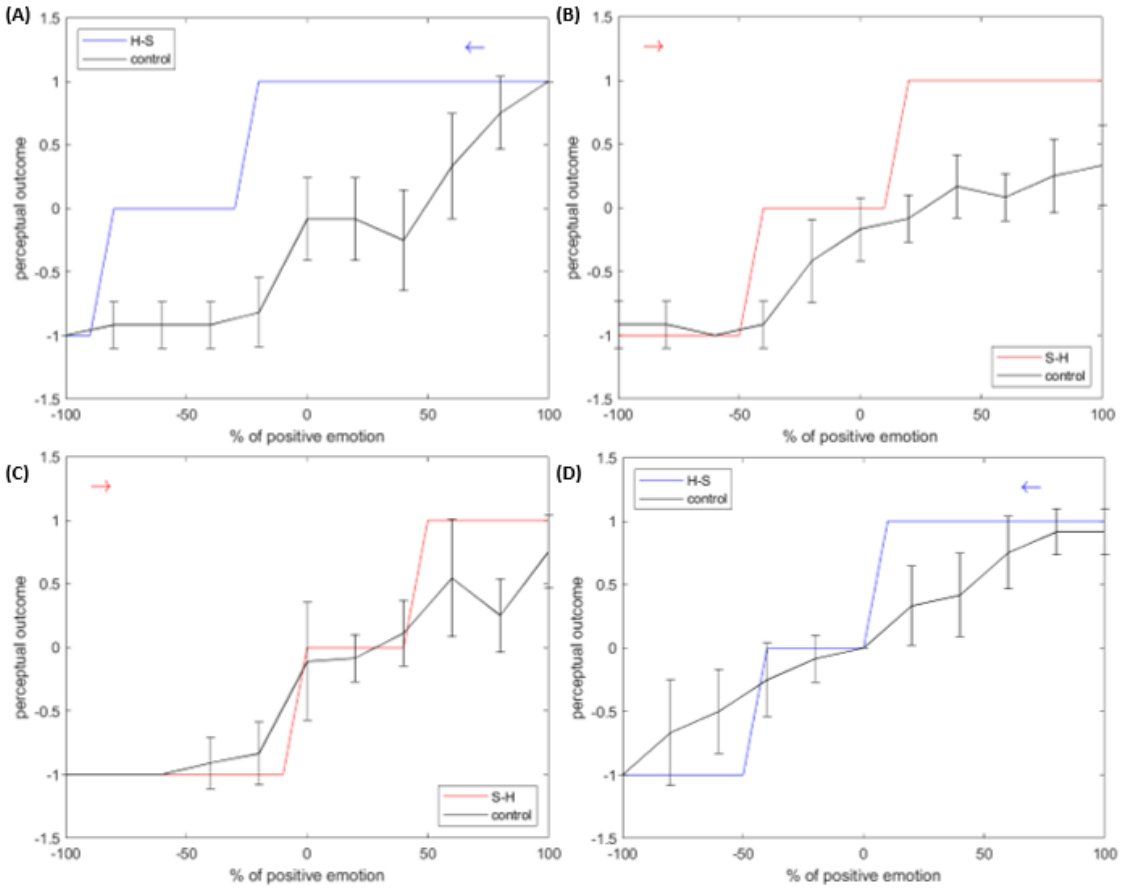

*Figure 18. Examples of classified trials according to the defined criteria: **(A) positive hysteresis**, characterized by a positive lag in the perception; **(B) negative hysteresis**, in which there is a negative lag in the perception; **(C) Null**, corresponding to the trajectories without hysteresis; **(D) Undefined**, which groups the trajectories with a behaviour different from what we expected for either positive or negative hysteresis. In the y-axis, -1 represents sadness, 0 the neutral state and 1 happiness, while in the x-axis, -100% is sadness, 0 neutral and 100% happiness.*

Finally, we added a quality visual expert review based on visual classification. The visual classification was performed by two independent raters individually at first and then discussing the cases of disagreement until reaching consensus. The visual expert classification always prevailed over classification derived from the mathematical criteria whenever they were not concordant.

2.2.2.2. Classifications of the individual trajectories

The two raters were given the examples of hysteresis curves well known from physics as well as examples of the four possible classifications and based their classification on that.

Table 12. Comparison of the visual classifications obtained by the 2 raters. There was an agreement on 635 of the 685 classifications, which corresponds to 92,7% of the trajectories and translates into a kappa Cohen of 0.88.

		Rater 1				
		NH	**PH**	**UN**	**N**	**Total**
Rater 2	**NH**	**152**	1	6	9	168
	PH	0	**348**	0	0	348
	UN	8	7	**64**	1	80
	N	12	5	6	**66**	89
	Total	172	361	76	76	685

The comparison between both classifications resulted in a total of 55 cases of disagreement out of a total of 685 trajectories, which translates in a kappa Cohen of 0.88 (Table 12). The cases of disagreement were then revised and discussed until reaching an accordance.

Using the criteria previously described, we performed the classification of the trajectories on having or not having hysteresis, and in the cases of hysteresis, what type it was.

Table 13 compares between the classifications reached using the criteria and the visual classification.

Table 13. Classifications results based on the criteria mentioned above and the results after visual revision. The visual classification prevailed over the classification with the criteria.

		CLASSIFICATION WITH THE CRITERIA				**AFTER VISUAL REVIEW**			
		NH	**PH**	**UN**	**Null**	**NH**	**PH**	**UN**	**Null**
Actor 2	Happy to Sad	46	89	9	11	24	105	9	17
	Sad to Happy	107	41	7	13	62	53	18	35
Actor 3	Happy to Sad	56	74	0	54	41	101	31	11
	Sad to Happy	70	74	29	5	32	89	31	26
Total		279	278	45	83	159	348	89	89

Although positive hysteresis seems to be overall predominant, the direction ‘sad to happy’ seems to have a proportion closer to an equilibrium between negative and positive hysteresis, with actor 2 having even more cases of negative hysteresis then positive hysteresis. These results are in accordance to the graphs of the group average where we could observe a prevalence of positive hysteresis in both actors, with actor 2 having the direction ‘sad to happy’ closer to the control curve in the second part of the trajectory.

Table 14. Results of the final classifications separated by subject.

		Actor 2				Actor 3			
Subject	**Direction**	NH	PH	UN	Null	NH	PH	UN	Null
01	Happy to Sad	2	4	2	1	2	4	0	2
	Sad to Happy	5	0	1	3	4	0	5	0
02	Happy to Sad	0	8	0	1	0	6	3	0
	Sad to Happy	0	2	1	6	1	2	4	1
03	Happy to Sad	0	1	1	0	0	5	2	1
	Sad to Happy	0	5	2	0	0	7	0	1
04	Happy to Sad	1	2	1	0	1	5	0	3
	Sad to Happy	5	1	0	2	5	0	0	3
05	Happy to Sad	0	2	0	0	0	4	4	0
	Sad to Happy	1	3	0	0	1	3	4	0
06	Happy to Sad	0	5	1	0	4	3	2	0
	Sad to Happy	0	7	0	0	0	2	7	0
07	Happy to Sad	8	0	0	0	1	8	0	0
	Sad to Happy	0	9	0	0	0	4	0	4
08	Happy to Sad	0	6	0	3	7	2	0	0
	Sad to Happy	0	2	0	7	1	7	0	0
09	Happy to Sad	1	4	0	2	3	4	1	1
	Sad to Happy	8	0	1	0	0	4	4	1
10	Happy to Sad	0	6	0	0	0	5	1	0
	Sad to Happy	4	0	1	0	0	4	0	2
11	Happy to Sad	0	1	4	4	6	0	2	1
	Sad to Happy	0	7	2	0	0	7	1	0
12	Happy to Sad	5	4	0	0	1	5	2	0
	Sad to Happy	0	7	0	0	0	8	0	0
13	Happy to Sad	1	7	0	1	0	5	4	0
	Sad to Happy	7	0	0	2	0	6	2	1
14	Happy to Sad	4	3	0	0	0	6	0	1
	Sad to Happy	1	2	1	3	4	0	1	2
15	Happy to Sad	0	7	0	0	1	4	4	0
	Sad to Happy	2	2	2	3	0	9	0	0
16	Happy to Sad	1	7	0	0	4	5	0	0
	Sad to Happy	8	0	0	1	8	1	0	0
17	Happy to Sad	0	2	0	0	0	6	0	0
	Sad to Happy	1	3	0	1	1	6	0	0
18	Happy to Sad	0	8	0	0	0	8	0	0
	Sad to Happy	7	0	0	0	2	0	0	4
19	Happy to Sad	1	6	0	1	4	4	1	0
	Sad to Happy	5	2	0	1	1	7	0	1
20	Happy to Sad	0	8	0	1	0	6	2	0
	Sad to Happy	4	1	0	1	0	6	0	1
21	Happy to Sad	0	5	0	3	5	1	3	0
	Sad to Happy	3	0	3	3	0	4	0	5
22	Happy to Sad	0	9	0	0	2	5	0	2
	Sad to Happy	1	0	4	2	4	2	3	0

The results of the classification of the trajectories per subject, presented in Table 14, allows us to better study the presence of such high number of cases of negative hysteresis. This sort of distribution shows heterogeneity, that was not apparent in the initial distributional analysis. We observe however, that while positive hysteresis seems to be consistently predominant in the direction 'happy to sad', there are several cases where negative hysteresis is predominant in the direction 'sad to happy' for both actors, which is in accordance to the happiness bias effect.

Table 15. Data used in the chi-square test for actor 2.

		Type of hysteresis		Total
		NH	PH	
Directions	Happy to sad	24	105	129
	Sad to Happy	62	53	115
Total		86	158	244

Table 16. Data used in the chi-squared test for actor 3.

		Type of hysteresis		Total
		NH	PH	
Directions	Happy to sad	41	101	142
	Sad to Happy	32	89	121
Total		73	190	263

Table 17. Data used in the chi-squared test for both actors.

		Type of hysteresis		Total
		NH	PH	
Directions	Happy to sad	65	206	271
	Sad to Happy	94	142	236
Total		159	348	507

Table 18. Chi-square test results using the total number of cases of positive and negative hysteresis for each actor and for both actors combined, after the visual review.

	df	N	Value	Asymptotic Sig. (2-sided test)
Actor 2	1	244	33,211	< 0,001
Actor 3	1	263	0,192	0,661
Both actors	1	507	14,713	< 0,001

To better understand if the type of hysteresis, negative or positive, depends on the direction, we performed a chi-square test (Table 18). Compiling the results from both actors (Table 17), there is a dependence of both variables studied, therefore the type of hysteresis depends on the direction taken which clearly manifests an effect of the history in the trajectory.

2.2.2.3. Inferential Statistical Analysis

For each direction, the trajectories were separated accordingly to the previous classification into two different distributions, one with negative hysteresis and other with positive hysteresis. To analyse the differences between these distributions we used two parameters: the perceptual switch moment for both classifications and the area between the two curves being compared.

These distributions were tested using the Shapiro-Wilk to assess whether they followed a normal distribution or not.

For the perceptual switch moments, all the distributions presented $p<0.05$ which confirms that the data do not follow a normal distribution (see Table 19). In general, the areas also did not follow a normal distribution with the exception of the direction 'sad to happy' of actor 3 and both directions of actor 2 (see Table 20). Therefore, we used non-parametric tests for the next part of the statistical analysis.

Table 19. Shapiro-Wilk test results for the distribution of the percentage of perceptual moment switch of the trajectory and the point of neutral state in the control curve.

			Statistic	df	Sig.
Actor 2	Happy to Sad	Positive hysteresis	0,939	105	< 0,001
		Negative hysteresis	0,888	24	0,012
	Sad to Happy	Positive hysteresis	0,928	53	0,004
		Negative hysteresis	0,937	62	0,003
Actor 3	Happy to Sad	Positive hysteresis	0,947	101	< 0,001
		Negative hysteresis	0,841	41	< 0,001
	Sad to Happy	Positive hysteresis	0,856	89	< 0,001
		Negative hysteresis	0,937	32	0,060

Table 20. Shapiro-Wilk test results for the distribution of the percentage of the areas between the control curve and the trajectory.

			Statistic	df	Sig.
Actor 2	Happy to Sad	Positive hysteresis	0,965	105	0,007
		Negative hysteresis	0,943	24	0,193
	Sad to Happy	Positive hysteresis	0,959	53	0,070
		Negative hysteresis	0,957	62	0,029
Actor 3	Happy to Sad	Positive hysteresis	0,973	101	0,040
		Negative hysteresis	0,937	41	0,026
	Sad to Happy	Positive hysteresis	0,970	89	0,039
		Negative hysteresis	0,933	32	0,048

We performed Mann-Whitney tests to assess the existence of statistically significant differences between both types of hysteresis (Table 13).

Table 21. Mann-Whitney test results for the distribution of the percentage of perceptual moment switch of the trajectory and the point of neutral state in the control curve.

			Total N	Mann-Whitney U	Asymptotic Sig. (2-sided test)
Actor 2	Happy to Sad	Positive hysteresis	129	461	< 0,001
		Negative hysteresis			
	Sad to Happy	Positive hysteresis	115	2509,5	< 0,001
		Negative hysteresis			
Actor 3	Happy to Sad	Positive hysteresis	142	166	< 0,001
		Negative hysteresis			
	Sad to Happy	Positive hysteresis	121	2647	< 0,001
		Negative hysteresis			

The results from Mann-Whitney tests for the perceptual switch moments comparison reveal significant differences between both types of hysteresis for both directions (see Table 13) for the two actors (Table 21).

Table 22. Mann-Whitney test results for the distribution of the percentage of the areas between the control curve and the trajectory.

			Total N	Mann-Whitney U	Asymptotic Sig. (2-sided test)
Actor 2	Happy to Sad	Positive hysteresis	129	1585	0,046
		Negative hysteresis			
	Sad to Happy	Positive hysteresis	115	2097	0,010
		Negative hysteresis			
Actor 3	Happy to Sad	Positive hysteresis	142	3378,5	< 0,001
		Negative hysteresis			
	Sad to Happy	Positive hysteresis	121	1890	0,006
		Negative hysteresis			

Mann-Whitney tests also revealed significant differences between the areas under trajectories of both types of hysteresis for both directions (see Table 13), 'happy to sad' and 'sad to happy', for the two actors (Table 22).

2.3. Discussion of Results

The present experiment was conducted to investigate the effect of the dynamic temporal context in the perception of emotions using biological motion stimuli by creating dynamic transitions between two emotions, happiness and sadness.

Biological motion perception is heavily influenced by our own experience in daily life social interactions as would be expected. This expected variability translates into the number of completed trajectories varying from participant to participant (Table 5) as well as the neutral point changing between participants (Table 7). In general, even for actor 1, which presented more ambiguous emotional expressions, the participants were able to easily identify the emotions through the biological motion stimuli and to see the transitions between the three emotions without major problems.

The perception of emotions on the dynamic transitions was significantly different than that on the control curves traced for each participant, proving that history does affect emotion perception, and therefore showing evidence of perceptual hysteresis.

At the descriptive group level positive hysteresis is predominant (Figure 16) which is in accordance with prior studies done with facial expressions. [29], [46], [48]. At the individual level, although positive hysteresis is still predominant in general, there are several cases of negative hysteresis and in some subjects it is even predominant (Table 14). The positive lag in the emotion perception present in these trajectories is explained by short-term memory mechanisms that help stabilizing a percept, reducing the ambiguity and therefore resulting in the persistence of that same percept.

Literature describes a happiness bias in the recognition of emotions from facial expressions. [29], [46], [47], [50], [51] This often leads to a persistence, or positive hysteresis, in trajectories where the first emotion is happiness when using face expressions as the stimuli. We did observe a prevalence of positive hysteresis, with about 61% of the cases being classified as such in the direction 'happy to sad', which is statistically significant as shown by the chi-squared test results (Table 18). However, we

observed that about 19% of the trajectories in this direction present negative hysteresis (Table 13). Negative hysteresis is normally attributed to adaptation mechanisms, that favour the switch to the other percept earlier than the physical transition happens in reality.

Recently, Ross *et al.* studied the effect of the use of masks on the recognition of emotions and concluded that when the body was shown there was not a big impact in performance, which suggests that biological motion perception plays role in the recognition of emotional states, only in the absence of facial expression information. They did however, observe that the recognition of happiness was significantly decreased in these cases. [54] This might explain the presence of a significant number of negative hysteresis in the present study: if the recognition of happiness on biological motion is not as strong, the happiness bias might not be as strong as well in the perception of our stimuli which will lead to the existence of trajectories with adaptation.

Interestingly, in the 'sad to happy' direction, although positive hysteresis is still predominant, the presence is much weaker, with about 41% of the trajectories presenting positive hysteresis and about 27% presenting negative hysteresis. In actor 2, negative hysteresis even surpasses it, with 37% of the total trajectories presenting negative hysteresis while 32% presents positive hysteresis (Table 13). In fact, chi-square tests reveal a statistically significant difference in the proportion of cases of positive and negative hysteresis depending on the direction of the stimuli (Table 18). This equilibrium of the cases might be a result of the effect of the happiness bias that favours the earlier perceptual switch to the happy percept.

Comparing trajectories with positive hysteresis and trajectories with negative hysteresis, Mann-Whitney tests revealed significant differences which supports our conclusion that perceptual hysteresis exists in biological motion perception.

The presence of trajectories with negative and positive hysteresis in the same direction in some participants reveals a possible competition between the short-term memory and adaptation mechanisms with short-term memory mostly overruling adaptation, which is in accordance to our hypothesis.

Chapter 3. MRI Experiment

3.1. Methods

3.1.1. fMRI data acquisition

The structural and functional MRI data were acquired at the Institute of Nuclear Sciences Applied to Health (ICNAS), Coimbra, Portugal, with a 3 Tesla Siemens Magnetom scanner with a 64 channel RF emitter-receiver head coil.

Every session started with the acquisition of one structural image, a T_1-weigthed Magnetization-Prepared Rapid Gradient-Echo (MPRAGE) sequence, followed by six functional runs using a T_2^*-weighted gradient echo-planar imaging (EPI) sequence, both with whole-brain coverage. The specific parameters for both types of image acquisitions are specified on Table 23.

The six functional runs consisted of 3 dynamic runs and 3 control runs interleaved. We acquired 486 volumes for the dynamic runs and 513 volumes for the control runs. Each session had the approximate duration of 45 minutes.

Table 23. Parameters used for the fMRI data acquisition.

	Structural Image Acquisition Parameters	Functional Image Acquisition Parameters
Repetition time (TR)	2530 ms	900 ms
Echo time (TE)	3.5 ms	37.00 ms
Flip angle (FA)	7º	68º
Voxel size	2.5 x 2.5 x 2.5 mm	2.5 x 2.5 x 2.5 mm
Field of view (FOV)	256 x 256 mm	200 x 200 mm
Number of slices	176	60

3.1.2. Experimental Design

The MRI experiment follows the same design as the behavioural experiment described in Chapter 2, with 3 runs of dynamic transitions and 3 runs of the control conditions. However, due to the results obtained for the previous experiment, we decided not to use the transitions of actor 1 in the fMRI experiment since this actor has been shown to be more ambiguous than the other two and therefore not as helpful to study the phenomenon of hysteresis which is the focus of this project.

The total number of the trials for each actor remained the same in both experiments, however the fixation cross time between trials and blocks is longer, having a duration of 11.7 seconds, for both the control and the dynamic runs to serve as baseline for the fMRI data analysis.

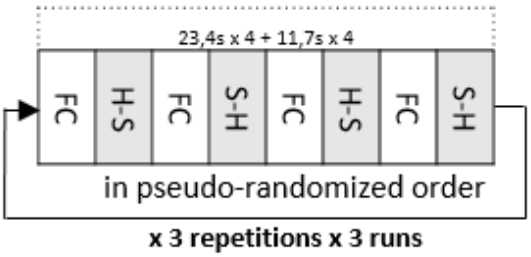

Figure 19. Experimental design for the dynamic trials, each run consisting of 3 blocks of 4 trials each, with a total duration of 7,22 minutes per run.

Each run of dynamic transitions consisted of 3 blocks of 4 trials each. Each stimulus had the duration of 22.6 seconds followed by a black screen during 0.8 seconds that results in a total of 23.4 seconds per trajectory followed by a fixation cross with the duration of 11.7 seconds which resulted in 35.1 seconds per trial. At the beginning and the end of the run it was presented a fixation cross for 11.7 seconds. In total each of these runs had the duration of approximately 7.22 minutes.

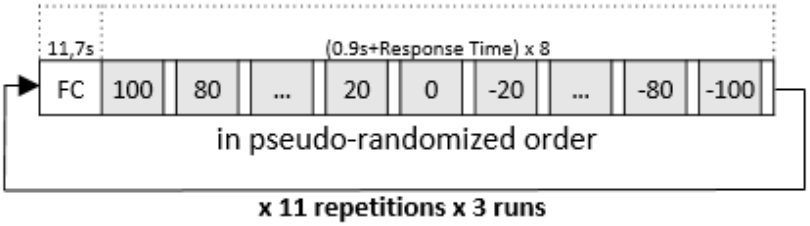

Figure 20. Experimental design for the control trials, each run consisting of 11 blocks of 8 trials each, with a total duration of 7,6 minutes per run.

The runs with the control conditions consisted of 11 blocks of 8 trials with a fixation cross of 11.7 seconds between blocks and the beginning and end of each run. Each stimulus had the duration of 0.9 seconds, which corresponds to a single step, followed by a black screen during which the participant reported the emotion perceived. This black screen had a duration of 1.8 or 2.7 or 3.6 seconds. This results in blocks with durations between 20.7 and 22.5 seconds. Each control run has the duration of approximately 7.6 minutes.

The rationale of the variable fixation duration of this design, which is called jittering, is to do a signal decomposition (deconvolution). If we started sampling always with the same time interval, all regions would be sampled in the same precise time from the start of the stimuli. This is particularly troublesome when the TR is short, which is the case of this design in which TR is 0.9 seconds, because we can miss signal since it is such a short time. Varying the times of response, we create a variation in the sampling process which allows to capture signal in each brain region at different times. [98]

In total, the functional acquisition had the duration of 44.5 minutes.

3.1.3. Participants

The group of participants for the fMRI experiment was the same group from the behavioural experiment. As of the writing of this thesis, we have not yet completed all the data acquisitions, therefore the data presented in this chapter correspond only to the four subjects that have already been scanned and analysed.

All participants provided written informed consent prior to the experiment following protocols approved by the Ethics Committee of the Faculty of Medicine of the University of Coimbra, in accordance with the Declaration of Helsinki.

Table 24. Information of the volunteers that participated in the fMRI acquisition until the moment of the writing of this thesis. These participants also take part on the behavioural experiment.

ID	Correspondent ID in the behavioural experiment	Age	Gender	Dominant Hand	Dominant eye	Laterality
sub-01	13	26	F	R	L	R
sub-02	05	22	F	R	R	R
sub-03	02	22	F	R	R	R
sub-04	21	22	M	R	R	R

3.1.4. Instructions

The instructions given to the participants were the same as in the behavioural experiment (see section 2.1.4), with the exception that this time there are no keys to press on the keyboard. Instead, there is an MR-compatible response box with four buttons. At the beginning of the acquisition of each run, the participant was asked to choose a key to associate to each of the three emotions.

After the fMRI acquisition, the participants were asked to answer the Portuguese version of the Positive and Negative Affect Schedule (PANAS-VRP) [102] regarding how they felt during the day. This scale allows us to obtain a value for both positive and negative emotions in order to assess how the mood of the participant was in the day of the acquisition, which is an aspect for future analysis.

3.2. Pre-processing fMRI data

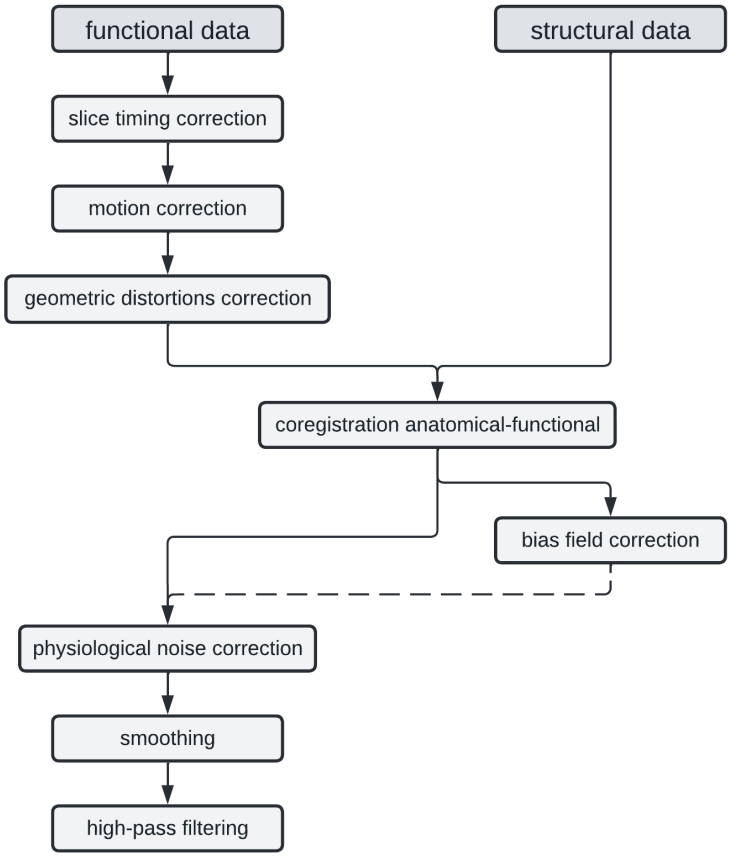

Figure 21. Pipeline used for the pre-processing of the fMRI data acquired.

The pre-processing steps (Figure 21) aim to create better quality images from the raw MRI data, improving the resolution and reducing the noise, by removing artefacts, and to validate model assumptions. Noise is created during the acquisition caused by head motion, random drifts, the heart beating and breathing. For both pre-processing the data and performing first-level and second-level analysis, we used *SPM12* in *Matlab*.

It is useful to assume that all the voxels in the image were acquired simultaneously. However, in EPI sequences, there is an interval of time between the acquisition of each slice corresponding to the TR, meaning that two successive slices are acquired with an interval of TR seconds. We can estimate the intensity of each voxel if they were all acquired at the same time by interpolating the signal intensity of that voxel in both the previous and the subsequent acquisitions in that point in time. This process is called slice-time correction. [96]

The next step is to correct the motion which consists in correcting the misalignments between the volumes caused by the movement of the head during the acquisition. Realignment comprises two steps: first it is made an estimation of how much each volume is misaligned in reference to either the mean of the volumes or to the first volume, and then it is made the re-slicing which uses the previously made estimations and moves each volume into the correct place. [96]

During the acquisition of EPI sequenced images, a susceptibility induced field is created, being constant in the set of functional images acquired but not matching with the structural image acquired. To correct these distortions, it is possible to estimate this field that maximizes the similarities between the volumes thus allowing us to obtain the corrected image. This step was implemented in FSL. [103], [104]

For the coregistration it is assumed that there is little to no movement of the head between the structural and functional images. Therefore, using four types of linear transformations, zooms, shears, rotations and translations, it is possible to move the source image over the reference image to align both images without introducing big errors in the data. The two images are first aligned by their outlines using the information of the positions of the gyrus, ventricles and sulcus, and then they are overlapped using the information of the contrasting areas that are known to be the same areas in both images (for example, the dark spots in the structural image which are the spaces filled with cerebrospinal fluid (CSF) correspond to lighter spots in the functional images) and moved around to achieve the best fit possible. The structural image is normally chosen as the source image and the functional image as the reference image as to not create unnecessary modifications in the functional image which is the image we want to analyse. [96]

The next step is the segmentation which consists of the mapping of different types of tissues. *SPM* recognizes six types of different tissues: the white matter, the grey matter, the CSF, soft tissue, bones and other tissues which comprised the areas of tissue not included in the other categories, including abnormal tissue. After the segmentation, it is possible to obtain a bias corrected image of our structural image which is an image with uniform intensities across the different types of tissues. This segmentation is particularly useful for the normalization process to the standard MNI space which was performed afterwards when preparing for the group level analysis as we kept all the images in the native space for the subject-level analysis for more accurate results. [96]

The respiration and cardiac fluctuations are responsible for a large part of the BOLD signal. [105] Using the measures of respiration and cardiac pulsation during the acquisition, it is possible to model the physiological noise. Using this model, we can correct the fMRI data extracting the effect the physiological noise has on the brain signal. For this step we used *Matlab PhysIO Toolbox*. In the cases where the physiological signal recording was compromised during the acquisition, we used only the Principal Components Analysis (PCA) performed using this toolbox as well. [106], [107]

The final step of the pre-processing is smoothing the images, aiming to increase the signal-to-noise ratio, by replacing the signal values in each voxel with the weighted average of the neighbouring voxels. [96]

3.3. Results

3.3.1. Subject level analysis

For the single subject analysis, we performed a General Linear Model (GLM) in the native space of each subject. GLM uses one or more variables, called regressors (X), to fit a model of the data to the measured signal (Y), and estimates beta weights (β) for all the regressors, assuming the data can be modulated using linear combinations of each regressor. The GLM is performed voxel-wise for each voxel time series, and each beta weight represents the contribution of the corresponding regressor for explaining the signal variation.

Mathematically, the brain responses to stimuli conditions are the result of the convolution of mathematical functions that model the well-known hemodynamic responses of the brain. The hemodynamic response is modulated by the neurovascular coupling. A predictor time course, or the ideal time series, is obtained as the result of the convolution of a box-car function (one for each regressor in the GLM) with a standard hemodynamic response function (HRF). The beta weights of the predictors of the ideal time series, associated with each condition, are then estimated to obtain the closest fit possible to the real time-series for each voxel (Y), based on the equation:

$$Y = \beta_1 X_1 + \beta_2 X_2 + \beta_3 X_3 + \cdots + \varepsilon$$

It is added an error factor (ε) to account for the discrepancies between both time-series caused by noise fluctuations.

With these parameters estimated, we can then make comparisons by creating contrasts, that consist of linear combinations of the beta values calculated.

We separated the data in different conditions based on the classifications of the trajectories for the dynamic transitions and on the classifications of emotions given in the control runs.

The classification of the trajectories followed the same steps as the trajectories obtained in the psychophysics experiment (see section 2.2.2.2), except the information was not divided per actor nor per direction, as our interest was to investigate the brain areas activated by each mechanism of hysteresis.

The final results of the classifications after visual review are presented in

Table 25. For this part, there was one visual rater, and another will be added in the future.

Table 25. Classifications of the trajectories of all the subjects that participated in the MRI experiment.

	NH	PH	UN	N	Invalids
sub-01	21	9	1	4	1
sub-02	6	16	0	0	14
sub-03	21	9	1	4	1
sub-04	13	14	0	8	1
Total	**61**	**48**	**2**	**16**	**17**

Given the low number of acquisitions so far, we can only make preliminary conclusions, based on the description of the results obtained. There is an equilibrium between cases of positive hysteresis and negative hysteresis, with negative hysteresis being surprisingly predominant at group level, possibly because of the new stimulation conditions.

We used all of the conditions in the dynamic transitions, independently of the attributed classification, and all of the periods of the control conditions, independently of the emotion perceived, to create a movement condition (MOV) in both runs. This condition and the periods of the fixation cross (FIX) were used to obtain activation maps for the contrast MOV-FIX for both the dynamic transitions and the control conditions (Figure 22).

According to the *SPM* radiological convention, the activation maps present the left side of the brain in the right side of each figure and vice-versa.

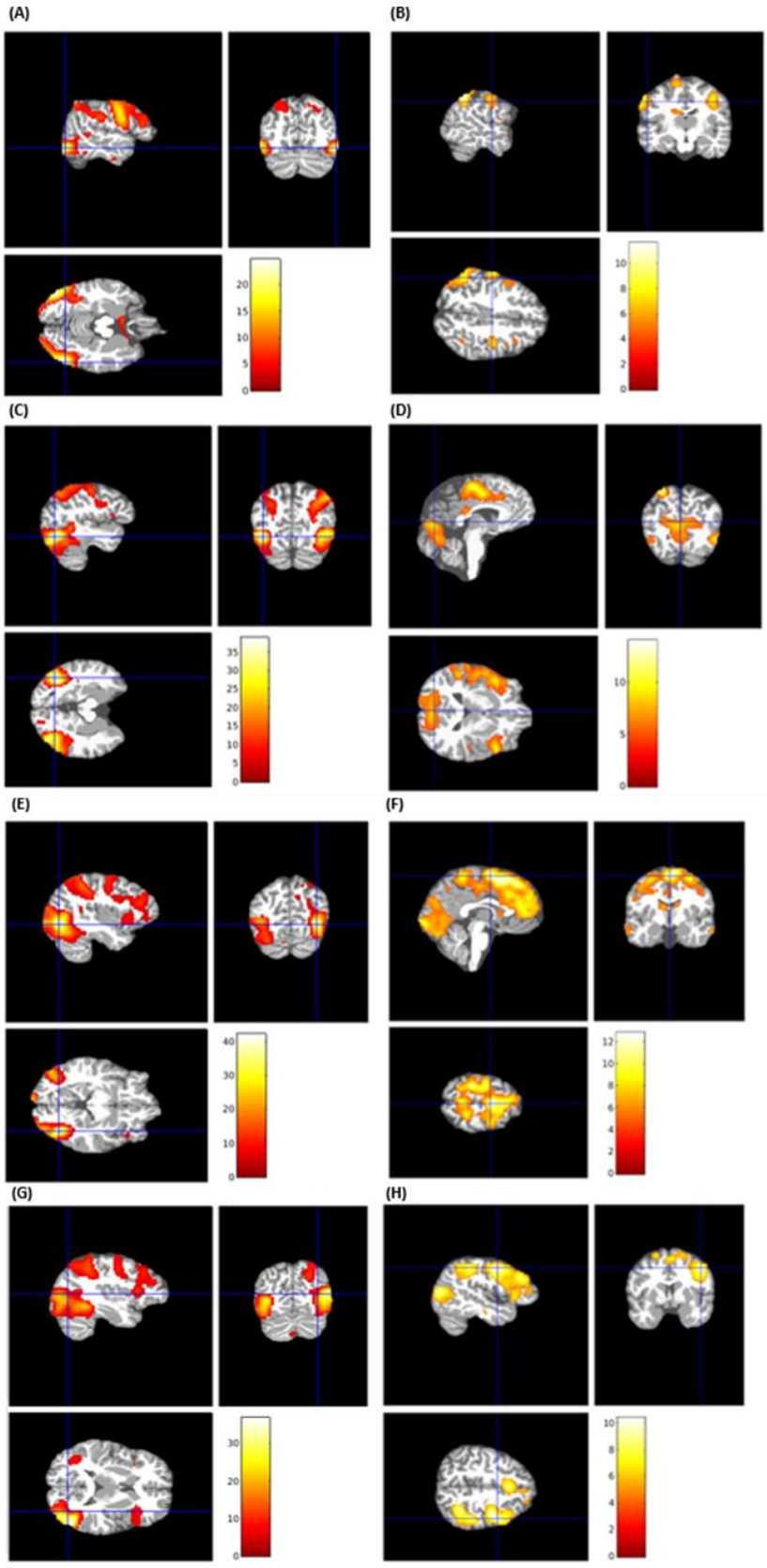

Figure 22. Activation maps resulting from contrasting movement (MOV) and fixation (FIX) for the dynamic transitions on the left column [(A) sub-01; (C) sub-02; (E) sub-03; (G) sub-04] and for control conditions on the right column [(B) sub-01; (D) sub-02; (F) sub-03; (H) sub-04] ($p < 0.05$ corrected).

For the control condition maps, shown in the right column of the Figure 22, sub-03 (Figure 22 (F)) presents a mostly symmetric activation map presenting very strong activations in the MT+ complex on both sides as well as insula. However, in the other three subjects there seems to exist a lateralization effect, with sub-01 (Figure 22 (A)) and sub-02 (Figure 22 (D)) presenting activity mostly in the left hemisphere, with strong clusters of activation in MT+ complex, the temporal lobe and cerebellum, and sub-04 (Figure 22 (H)) showing stronger activity on the right hemisphere, mostly in the MT+ complex and the insula.

Interestingly, this lateralization effect is not so apparent in the dynamic transitions, as seen in the left column of the Figure 22, especially regarding MT+ complex which presents strong activity in both sides for all the subjects. As expected, we can also observe strong activations in insula, which is involved in the decision-making as well as in emotion perception; the SPL, related with the biological motion perception; as well as activations in PCF and DLPFC related with the decision-making.

We then proceeded to create two contrasts to compare both types of hysteresis, positive hysteresis (PH) and negative hysteresis (NH), based on the initial classification. The first contrast NH-PH consisted in the activation map that results from the subtraction of the periods of positive hysteresis to the periods of negative hysteresis, and the second contrast, PH-NH, consists of the opposite.

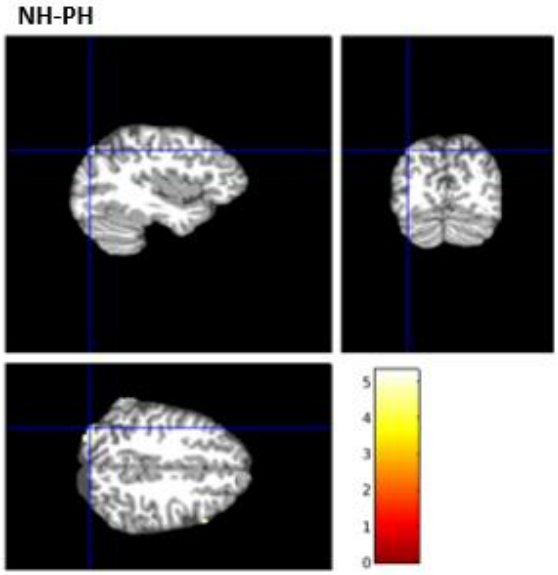

Figure 23. Activation map for the contrast NH-PH for sub-01 (p < 0.05 corrected).

Using the contrast NH-PH for sub-01 (Figure 23) results in only two small clusters of activation located in the parietal lobe and in the PFC. As for the contrast PH-NH it was not possible to observe any activated areas.

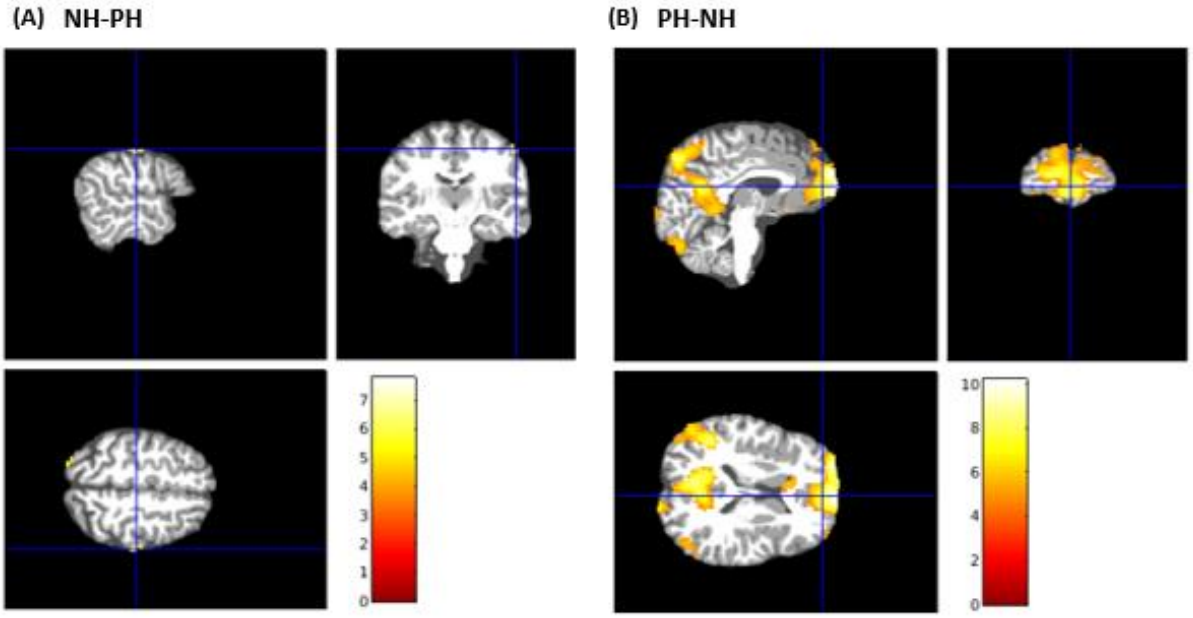

Figure 24. Activation maps for the contrast NH-PH, on the left (A), and for the contrast PH-NH, on the right (B), for sub-02 (p < 0.05 corrected).

Similarly, to the results obtained for sub-01 for the contrast NH-PH (Figure 24(A)), there are only two small clusters of activation in the map for sub-02 using this contrast, in the parietal and the temporal lobes. On the contrary, the contrast PH-NH (Figure 24(B)) results in a map of strong activations mostly on the left hemisphere, with a clear strong large cluster in the MT+ complex, as well as in the parietal lobe, the cerebellum and both right and left FEF.

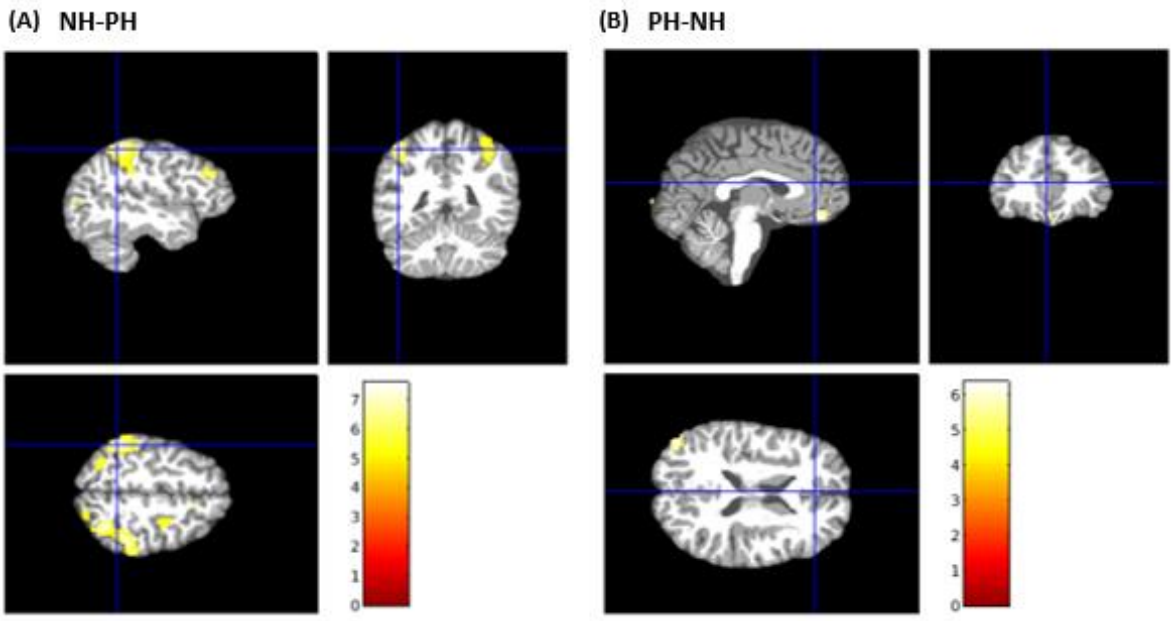

Figure 25. Activation maps for the contrast NH-PH, on the left (A,) and for the contrast PH-NH, on the right (B), for sub-03 ($p < 0.05$ corrected).

Contrary to the results obtained for sub-01 and sub-02, the contrast NH-PH for sub-03 (Figure 25(A)) results in a stronger activation map than the contrast PH-NH (Figure 25(B)). For the contrast NH-PH, there are clear activations in the MT+ complex as well as SPL in both hemispheres while for the contrast PH-NH there are only small clusters of activation in the parietal and frontal lobes.

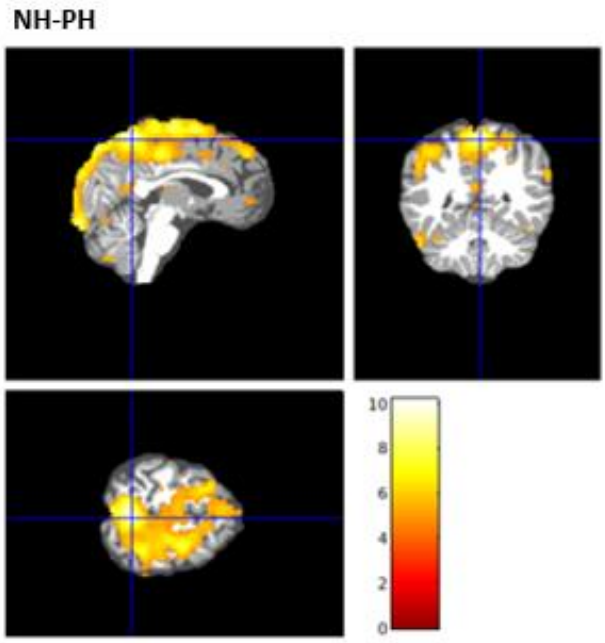

Figure 26. Activation map for the contrast NH-PH for sub-04 ($p < 0.05$ corrected).

For sub-04, using the contrast PH-NH it was not possible to observe any activated areas. As for the contrast NH-PH, there is strong activity in both hemispheres of the brain, with a relatively larger area of activity in the right side, as observed in Figure 26. We can observe strong activity in the SPL, the MT+ complex, right amygdala, right insula, both right and left PFC, FEF and the cerebellum.

3.3.2. Group level analysis

We performed a fixed-effects analysis (FFX) at group level, which is a statistic approach that takes the statistical maps obtained at subject level, accepting them as measures of the responses of each subject, and obtains a summary of those measures that are common across all subjects, allowing the creation of activation maps at group level that highlight brain areas activated in the task at study. One down-side of FFX is that it does not model the inter-subject variability for generalization to the population, only allowing to make conclusions for the specific sample that is being studied, making it a good choice for studying pilot data and small groups. [96]

For group analysis it is necessary that each voxel corresponds to the same spatial location across all the brains. Individual brains have features and shapes that distinguish them from each other. However, independently of how these differences, there are always

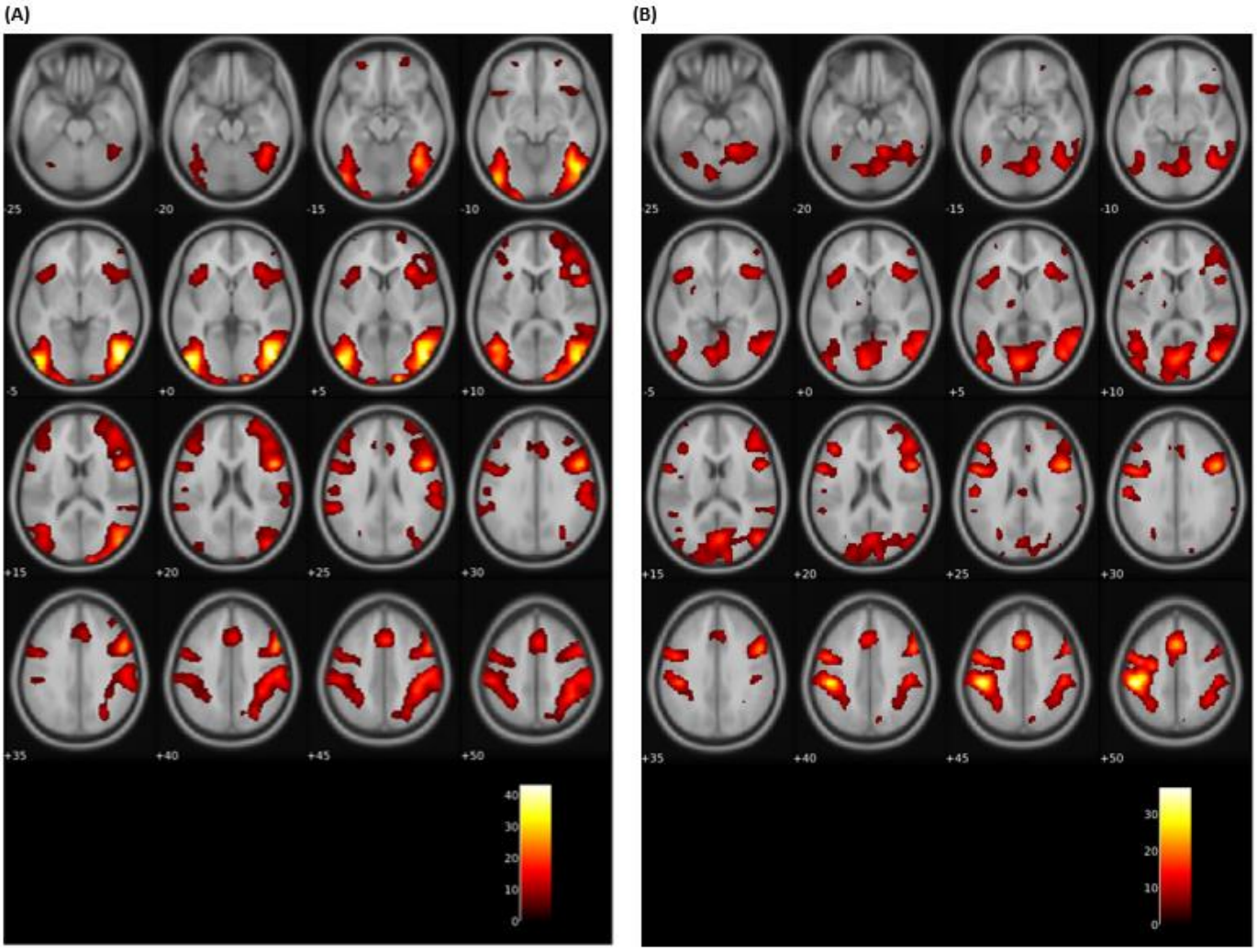

Figure 27. Contrast results between movement (MOV) and fixation (FIX) at group level for the dynamic transitions (A) and for the control conditions (B) with p < 0.05 corrected.

common features across all healthy brains. Therefore, it is possible to do a normalization, registering each of the individual brains to a standardized space, in this case the MNI space, that follows a pre-made template and allows for the comparison both at group level and across groups from other independent studies. [96]

Contrasting movement with fixation in the dynamic transitions (Figure 27(A)) and the control condition (Figure 27(B)), results in activation maps very similar to each other with strong activations in areas related with the processing of both biological motion and emotions as well as for percetual decision-making.

We can see several areas related to biological motion activated like the left and right vPMC and SMA, STS, SPL, cerebellum and the MT+ complex, the latter showing

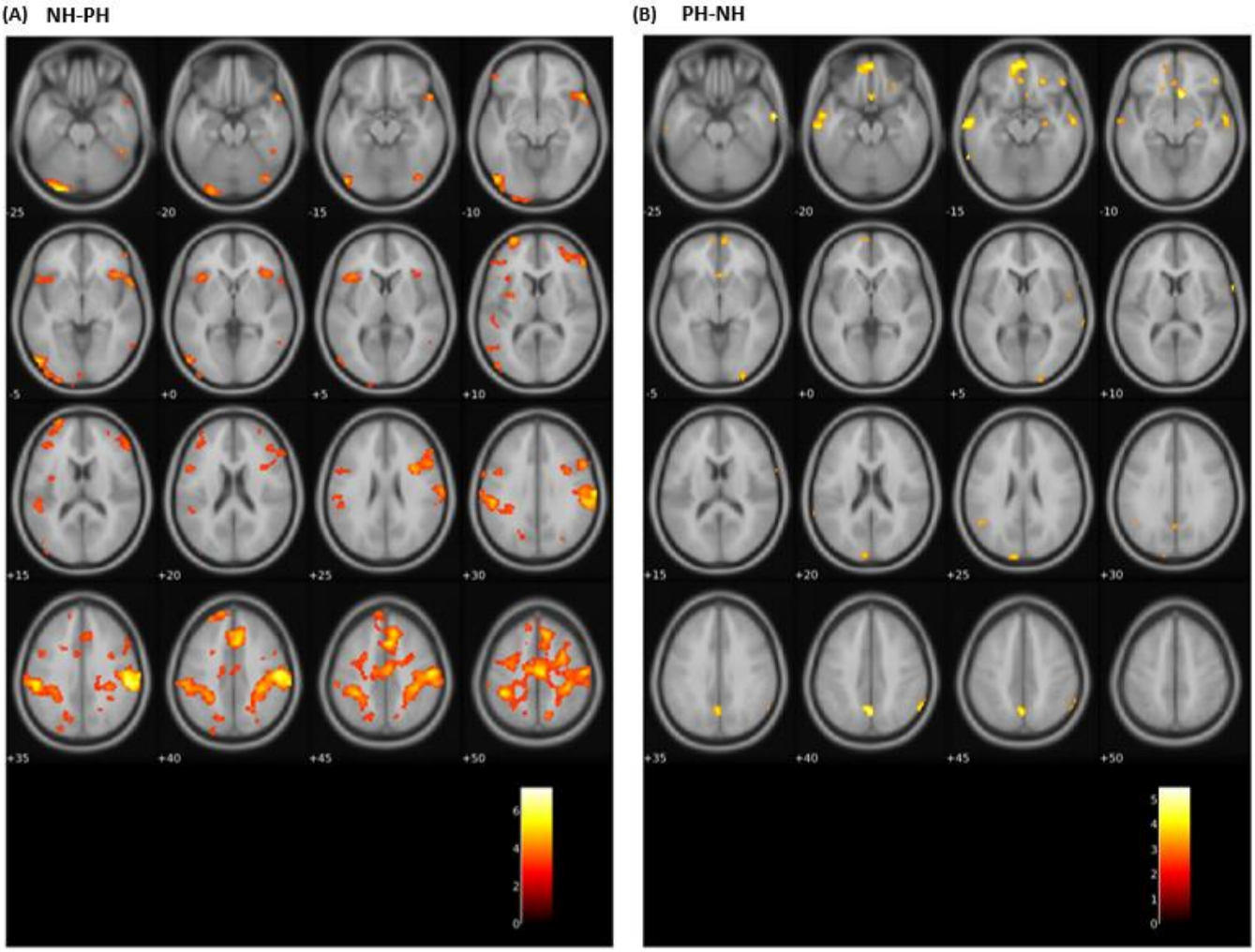

Figure 28. Brain areas activated when contrasting positive and negative hysteresis at group level (p<0.001 uncorrected).

stronger activity in the dynamic transitions (Figure 27(A)) in comparison to the control conditions (Figure 27(B)).

The emotion processing is responsible for the activation of areas such as right and left PFC, rigth and left insula, cerebellum, talamus and OFC.

Finally, we can distinguish areas such as the fusiform gyrus, the right and left DLPFC, right and left PFC, right and left FEF, right and left insula as well as both right and left primary somatosensory cortex that are known to contribute to the process of decision-making.

There are also clusters present in early visual areas such as secondary visual cortex and associative visual cortex.

While the contrast NH-PH (Figure 28(A)) results in an activation map with several strong clusters of activation, the contrast PH-NH (Figure 28(B)) only shows small clusters of activation in the frontal, temporal and parietal lobes.

The activation map for the negative hysteresis contrast shows clusters in areas well-known for the processing of biological motion, such as TPJ, STS, SPL, IPL, IFG, vPMC, SMA and cerebellum; of emotions, such as the PFC, both right and left insula, cerebellum and STS; and in perceptual decision-making, such as the PFC, DLPFC, dorsal PCC, both left and right primary somatosensory cortex, parahippocampal gyrus, fusiform gyrus, both right and left insula, FEF and IFG; as well as visual processing areas, the left secondary visual cortex and both right and left associative visual cortex.

As for the activation map for positive hysteresis, we can see very small clusters of activity in areas known for perceptual decision-making such as the dorsal PCC, the anterior PFC, FEF, IFG; for biological motion perception such as SPL, IFG and MT; for emotion processing, such as the anterior PFC, STS, cerebellum, the right hippocampus, and both right and left OFC; and for visual processing areas, including the left secondary visual cortex; as well as other areas in the parietal lobe, like the angular gyrus, and the temporal lobe.

3.4. Discussion of Results

At subject level, the activation maps obtained for the condition MOV-FIX in the dynamic transition runs and the control runs differ slightly intra-subject which was expected from the individual variability for high level perception. The major difference observed is the apparent lateralization in the control runs, with sub-01 and sub-02 presenting a left lateralization while sub-04 shows a right lateralization (Figure 22). Overall, all of the expected areas of activation given the nature of the stimulus and the task were present in both maps of activation, even if being unilateral activations in the control condition.

Although lateralization in the processing of emotions is a well-known phenomenon, there is still not a widely accepted explanation for it, with several different theories and models rising in the last years.[57], [108]–[112]

Markowitsch's theory defends that the left amygdala is responsible for the processing of emotional information associated with language and detailed features therefore being

responsible for processing high-level information regarding the emotions while the right amygdala oversees a fast and superficial analysis of the emotions, such as imagery associated with the emotional information.[108]

Phelps proposed a similar theory to Markowitsch's but expressed in simpler terms: the emotional information is processed in both sides of the brain, with the left amygdala being responsible for processing the information of verbal nature and communication and the right amygdala processing the visual and straightforward aspects of the emotions.[109]

On the other hand, Wright defended that the right amygdala adapts faster than the left amygdala, having, therefore, a quicker and more dynamic detection of the emotional stimuli while the left amygdala does a more prolonged and specialized evaluation of the emotional stimuli.[110]

Gläscher and Adolphus's model for emotion processing describes the right amygdala as the first to respond to emotional stimuli in a fast and automatic manner and mediating a global response while the left amygdala acts more specifically and later, mediating a longer response that aims to decode the variations of magnitude of the arousal provoked by the presented stimuli.[112]

Given the low number of cases we present here we cannot conclude if there is in fact a strong lateralization effect for emotion recognition from biological motion. Furthermore, we cannot say if existing that effect, it is explained by any of these theories. We can however, predict that the right lateralization observed in the these might be related to the visual nature of the stimulus while left activations could be related to the task itself with the need for subjects to engage in a higher-level processing of the emotional information to decode the variations of emotion over time and accomplish the task.

As for the results obtained using the contrasts with the two main conditions, positive and negative hysteresis, the activation maps at subject level reveal some heterogeneity over the four subjects: with sub-01 not revealing any activity for the contrast PH-NH but activations using the contrast NH-PH (Figure 23) while sub-04 does not reveal any activity in the contrast NH-PH but has a strong activation map for contrast PH-NH (Figure 26). Sub-02 has a stronger map for PH-NH (Figure 24) while sub-03 presents a stronger map for NH-PH (Figure 25). A possible explanation aside for inter-individual variability might lie in the imbalance in the number of trials for each condition, as described in

Table 25. The same explanation could perhaps be applied to the results at group level for these contrasts. While the contrast NH-PH results in a strong activation map, the contrast PH-NH shows very small clusters of activation (Figure 28).

At group level, the differences observed for the contrast MOV-FIX for the dynamic transitions and the control conditions seem to be attenuated (Figure 27). The lateralization effect seen in the control conditions in the individual activation maps does not appear in the group activation maps which was to be expected since there is no homogeneity in the lateralization effects among the subjects, which results in a cancelation of the effect in the group average. As expected, both maps show activation in areas previously described as associated with the nature of the stimulus, such as areas involved in the processing of biological motion, with particularly strong activity in the MT+ complex as well as the SPL, and of emotions, particularly cerebellum, STS and insula, as well as areas related with perceptual decision-making, with very strong clusters of activity in both maps in the insula, PFC and DLPFC.

For the activation maps obtained using the contrasts with both types of hysteresis, we observed a stronger and more extended map of activation for NH-PH in comparison to the one of PH-NH (Figure 28). The clusters obtained corresponded to areas associated with both the nature of the stimulus and the decision-making process. These differences cannot be interpreted as absolute differences between the networks activated by the two types of hysteresis given the low number of trials used for both conditions resulting of the low number of subjects in the experiment.

Chapter 4. Future work

At the moment of the writing of this dissertation, the MRI acquisitions are still in progress, but it is our goal to complete these acquisitions with the participation of the volunteers that have been included in the psychophysics experiment. After the completion of these acquisitions, we will then have the sufficient data to perform analysis at both subject and group level, following an approach similar to the one described in Chapter 3.

It is our goal to also use the acquired data to perform connectivity studies based on regions of interest determined in this first analysis to obtain information about the neural correlates and networks that underlie the mechanisms here described.

Even though the research on the healthy subjects is still ongoing for the MRI part of the project, the results from the behavioural experiment stated a clear presence of hysteresis in the perception of emotion in biological motion stimuli. This fact associated with the knowledge that the perception of both emotional and biological motion stimuli is severely compromised in neurodevelopmental disorders, such as autism and schizophrenia, leads to the question of whether these mechanisms are compromised in these disorders as well. The data collected in this project could be of use as a control group for a possible clinical investigation to answer that question.

References

[1] H. Ashida, A. Lingnau, M. B. Wall, and A. T. Smith, "fMRI adaptation reveals separate mechanisms for first-order and second-order motion," *J. Neurophysiol.*, vol. 97, no. 2, pp. 1319–1325, 2007, doi: 10.1152/jn.00723.2006.

[2] K. S. Weiner, R. Sayres, J. Vinberg, and K. Grill-Spector, "fMRI-adaptation and category selectivity in human ventral temporal cortex: Regional differences across time scales," *J. Neurophysiol.*, vol. 103, no. 6, pp. 3349–3365, 2010, doi: 10.1152/jn.01108.2009.

[3] J. Larsson, D. J. Heeger, and M. S. Landy, "Orientation selectivity of motion-boundary responses in human visual cortex," *J. Neurophysiol.*, vol. 104, no. 6, pp. 2940–2950, 2010, doi: 10.1152/jn.00400.2010.

[4] C. Brozzoli, G. Gentile, V. I. Petkova, and H. H. Ehrsson, "fMRI adaptation reveals a cortical mechanism for the coding of space near the hand," *J. Neurosci.*, vol. 31, no. 24, pp. 9023–9031, 2011, doi: 10.1523/JNEUROSCI.1172-11.2011.

[5] M. N. Shadlen and R. Kiani, "Decision making as a window on cognition," *Neuron*, vol. 80, no. 3, pp. 791–806, 2013, doi: 10.1016/j.neuron.2013.10.047.

[6] M. Siegel, A. K. Engel, and T. H. Donner, "Cortical network dynamics of perceptual decision-making in the human brain," *Front. Hum. Neurosci.*, vol. 5, pp. 1–12, 2011, doi: 10.3389/fnhum.2011.00021.

[7] C. Preuschhof, H. R. Heekeren, B. Taskin, T. Schubert, and A. Villringer, "Neural correlates of vibrotactile working memory in the human brain," *J. Neurosci.*, vol. 26, no. 51, pp. 13231–13239, 2006, doi: 10.1523/JNEUROSCI.2767-06.2006.

[8] B. Pleger, C. Ruff, F. Blankenburg, S. Bestmann, K. Wiech, K. Stephan, A. Capilla, K. Friston, and R. Dolan, "Neural coding of tactile decisions in the human prefrontal cortex," *J. Neurosci.*, vol. 26, no. 48, pp. 12596–12601, 2006, doi: 10.1523/JNEUROSCI.4275-06.2006.

[9] M. Petrides, "Deficits in non-spatial conditional associative learning after periarcuate lesions in the monkey," *Behav. Brain Res.*, vol. 16, no. 2–3, pp. 95–101, 1985, doi: 10.1016/0166-4328(85)90085-3.

[10] F. C. Donders, "On the speed of mental processes," *Acta Psychol. (Amst).*, vol. 30, pp. 412–431, 1969, doi: 10.1016/0001-6918(69)90065-1.

[11] J. R. Binder, E. Liebenthal, E. T. Possing, D. A. Medler, and B. D. Ward, "Neural correlates of sensory and decision processes in auditory object identification," *Nat. Neurosci.*, vol. 7, no. 3, pp. 295–301, 2004, doi: 10.1038/nn1198.

[12] M. Intaitė, J. V. Duarte, and M. Castelo-Branco, "Working memory load influences perceptual ambiguity by competing for fronto-parietal attentional resources," *Brain Res.*, vol. 1650, pp. 142–151, 2016, doi: 10.1016/j.brainres.2016.08.044.

[13] A. Thielscher and L. Pessoa, "Neural correlates of perceptual choice and decision making during fear-disgust discrimination," *J. Neurosci.*, vol. 27, no. 11, pp. 2908–2917, 2007, doi: 10.1523/JNEUROSCI.3024-06.2007.

[14] H. R. Heekeren, S. Marrett, P. A. Bandettini, and L. G. Ungerleider, "A general mechanism for perceptual decision-making in the human brain," *Nature*, vol. 431, pp. 859–862, 2004, doi: 10.1038/nature02966.

[15] S. J. Heinen, J. Rowland, B. T. Lee, and A. R. Wade, "An oculomotor decision process revealed by functional magnetic resonance imaging," *J. Neurosci.*, vol. 26, no. 52, pp. 13515–13522, 2006, doi: 10.1523/JNEUROSCI.4243-06.2006.

[16] P. Cisek and J. F. Kalaska, "Neural correlates of reaching decisions in dorsal premotor cortex: Specification of multiple direction choices and final selection of action," *Neuron*, vol. 45, no. 5, pp. 801–814, 2005, doi: 10.1016/j.neuron.2005.01.027.

[17] M. N. Shadlen and W. T. Newsome, "Motion perception: Seeing and deciding," *Proc. Natl. Acad. Sci. U. S. A.*, vol. 93, no. 2, pp. 628–633, 1996, doi: 10.1073/pnas.93.2.628.

[18] D. P. Hanes and J. D. Schall, "Neural control of voluntary movement initiation," *Science*, vol. 274, no. 5286, pp. 427–430, 1996, doi: 10.1126/science.274.5286.427.

[19] H. R. Heekeren, S. Marrett, D. A. Ruff, P. A. Bandettini, and L. G. Ungerleider, "Involvement of human left dorsolateral prefrontal cortex in perceptual decision making is independent of response modality," *Proc. Natl. Acad. Sci. U. S. A.*, vol. 103, no. 26, pp. 10023–10028, 2006, doi: 10.1073/pnas.0603949103.

[20] T. Egner and J. Hirsch, "Cognitive control mechanisms resolve conflict through cortical amplification of task-relevant information," *Nat. Neurosci.*, vol. 8, no. 12, pp. 1784–1790, 2005, doi: 10.1038/nn1594.

[21] D. C. Jiles and D. L. Atherton, "Theory of ferromagnetic hysteresis (invited)," *J. Appl. Phys.*, vol. 55, pp. 2115–2120, 1984, doi: 10.1063/1.333582.

[22] E. C. Stoner and E. P. Wohlfarth, "A mechanism of magnetic hysteresis in heterogeneous alloys," *Philos. Trans. R. Soc. London. Ser. A, Math. Phys. Sci.*, vol. 240, no. 826, pp. 599–642, 1948, doi: 10.1098/rsta.1948.0007.

[23] E. Warbrug, "Magnetische Untersuchungen [Magnetic investigations]," *Ann. Phys.*, vol. 249, no. 5, pp. 141-164, 1881.

[24] A. Buckthought, J. Kim, and H. R. Wilson, "Hysteresis effects in stereopsis and binocular rivalry," *Vision Res.*, vol. 48, no. 6, pp. 819–830, 2008, doi: 10.1016/j.visres.2007.12.013.

[25] H. S. Hock, J. A. S. Kelso, and G. Schöner, “Bistability and Hysteresis in the Organization of Apparent Motion Patterns,” *J. Exp. Psychol. Hum. Percept. Perform.*, vol. 19, no. 1, pp. 63–80, 1993, doi: 10.1037/0096-1523.19.1.63.

[26] H. R. Wilson, “Hysteresis in binocular grating perception: Contrast effects,” *Vision Res.*, vol. 17, no. 7, pp. 843–851, 1977, doi: 10.1016/0042-6989(77)90128-6.

[27] A. Kleinschmidt, C. Büchel, C. Hutton, K. J. Friston, and R. S. J. Frackowiak, “The neural structures expressing perceptual hysteresis in visual letter recognition,” *Neuron*, vol. 34, no. 4, pp. 659–666, 2002, doi: 10.1016/S0896-6273(02)00694-3.

[28] J. A. Assad, N. Hacohen, and D. P. Corey, “Voltage dependence of adaptation and active bundle movement in bullfrog saccular hair cells,” *Proc. Natl. Acad. Sci. U. S. A.*, vol. 86, no. 8, pp. 2918–2922, 1989, doi: 10.1073/pnas.86.8.2918.

[29] E. Liaci, A. Fischer, H. Atmanspacher, M. Heinrichs, L. Tebartz van Elst, and J. Kornmeier, "Positive and negative hysteresis effects for the perception of geometric and emotional ambiguities," *PLoS ONE*, vol. 13, no. 9. 2018. doi: 10.1371/journal.pone.0202398.

[30] A. N. Pisarchik, R. Jaimes-Reátegui, C. D. A. Magallón-García, and C. O. Castillo-Morales, “Critical slowing down and noise-induced intermittency in bistable perception: Bifurcation analysis,” *Biol. Cybern.*, vol. 108, pp. 397–404, 2014, doi: 10.1007/s00422-014-0607-5.

[31] C. M. Schwiedrzik, C. C. Ruff, A. Lazar, F. C. Leitner, W. Singer, and L. Melloni, “Untangling perceptual memory: Hysteresis and adaptation map into separate cortical networks,” *Cereb. Cortex*, vol. 24, no. 5, pp. 1152–1164, 2014, doi: 10.1093/cercor/bhs396.

[32] S. M. Lopresti-Goodman, M. T. Turvey, and T. D. Frank, “Negative hysteresis in the behavioral dynamics of the affordance ‘graspable,’” *Attention, Perception, Psychophys.*, vol. 75, pp. 1075–1091, 2013, doi: 10.3758/s13414-013-0437-x.

[33] A. Sayal, T. Sousa, J. V. Duarte, G. N. Costa, R. Martins, and M. Castelo-Branco, “Identification of competing neural mechanisms underlying positive and negative perceptual hysteresis in the human visual system,” *Neuroimage*, vol. 221, p. 117153, 2020, doi: 10.1016/j.neuroimage.2020.117153.

[34] K. F. Valyear, A. M. Fitzpatrick, and N. M. Dundon, “Now and then: Hand choice is influenced by recent action history,” *Psychon. Bull. Rev.*, vol. 26, no. 1, pp. 305–314, 2019, doi: 10.3758/s13423-018-1510-1.

[35] C. Schütz, M. Weigelt, and T. Schack, “Cognitive costs of motor planning do not differ between pointing and grasping in a sequential task,” *Exp. Brain Res.*, vol. 234, no. 7, pp.

2035–2043, 2016, doi: 10.1007/s00221-016-4608-6.

[36] C. Schütz, M. Weigelt, and T. Schack, "Motor hysteresis in a sequential grasping and pointing task is absent in task-critical joints," *Exp. Brain Res.*, vol. 235, no. 3, pp. 703–712, 2017, doi: 10.1007/s00221-016-4831-1.

[37] M. S. Rostoft, H. Sigmundsson, H. T. A. Whiting, and R. P. Ingvaldsen, "Dynamics of hand preference in 4 year-old children," *Behav. Brain Res.*, vol. 132, no. 1, pp. 59–68, 2002, doi: 10.1016/S0166-4328(01)00415-6.

[38] W. M. Land, D. A. Rosenbaum, C. Seegelke, and T. Schack, "Whole-body posture planning in anticipation of a manual prehension task: Prospective and retrospective effects," *Acta Psychol. (Amst).*, vol. 144, no. 2, pp. 298–307, 2013, doi: 10.1016/j.actpsy.2013.06.002.

[39] H. T. Weiler and F. Awiszus, "Influence of hysteresis on joint position sense in the human knee joint," *Exp. Brain Res.*, vol. 135, no. 2, pp. 215–221, 2000, doi: 10.1007/s002210000512.

[40] A. I. Kostyukov, A. V. Gorkovenko, Y. A. Kulyk, O. V. Lehedza, D. I. Shushuiev, M. Zasada, and S. S. Strafun, "Central Commands to the Elbow and Shoulder Muscles During Circular Planar Movements of Hand With Simultaneous Generation of Tangential Forces," *Front. Physiol.*, vol. 13, 2022, doi: 10.3389/fphys.2022.864404.

[41] B. M. Adhikari, K. M. Quinn, and M. Dhamala, "Is the Brain's Inertia for Motor Movements Different for Acceleration and Deceleration?," *PLoS One*, vol. 8, no. 10, 2013, doi: 10.1371/journal.pone.0078055.

[42] R. Burgess-Limerick, J. Shemmell, B. K. Barry, R. G. Carson, and B. Abernethy, "Spontaneous transitions in the coordination of a whole body task," *Hum. Mov. Sci.*, vol. 20, no. 4–5, pp. 549–562, 2001, doi: 10.1016/S0167-9457(01)00067-7.

[43] H. Kobayashi and F. Hara, "Dynamic recognition of 6 basic facial expressions by discrete-time recurrent neural network," *Trans. Jpn. Soc. Mech. Eng. C*, vol. 62, pp. 644–651, 1996, doi: 10.1299/kikaic.62.644.

[44] J. R. Martin, G. Dezecache, D. Pressnitzer, P. Nuss, J. Dokic, N. Bruno, E. Pacherie, and N. Franck, "Perceptual hysteresis as a marker of perceptual inflexibility in schizophrenia," *Conscious. Cogn.*, vol. 30, pp. 62–72, 2014, doi: 10.1016/j.concog.2014.07.014.

[45] M. A. Webster, D. Kaping, Y. Mizokami, and P. Duhamel, "Adaptation to natural facial categories," *Nature*, vol. 428, no. 6982, pp. 557-561, 2004, doi: https://doi.org/10.1038/nature02420.

[46] A. Verdade, J. Castelhano, T. Sousa, and M. Castelo-Branco, "How positive emotional content overrules perceptual history effects: Hysteresis in emotion recognition," *J. Vis.*,

vol. 20, no. 8, pp. 1–15, 2020, doi: 10.1167/JOV.20.8.19.

[47] A. Verdade, T. Sousa, J. Castelhano, and M. Castelo-Branco, “Positive hysteresis in emotion recognition : Face processing visual regions are involved in perceptual persistence , which mediates interactions between anterior insula and medial prefrontal cortex,” *Cogn. Affect. Behav. Neurosci.*, 2022, doi: 10.3758/s13415-022-01024-w.

[48] V. Sacharin, D. Sander, and K. R. Scherer, “The perception of changing emotion expressions,” *Cogn. Emot.*, vol. 26, no. 7, pp. 1273–1300, 2012, doi: 10.1080/02699931.2012.656583.

[49] N. Kanwisher, “Domain specificity in face perception,” *Nat. Neurosci.*, vol. 3, no. 8, pp. 759–763, 2000, doi: 10.1038/77664.

[50] T. Kirita and M. Endo, “Happy face advantage in recognizing facial expressions,” *Acta Psychol. (Amst).*, vol. 89, no. 2, pp. 149–163, 1995, doi: 10.1016/0001-6918(94)00021-8.

[53] H. Lee and J. Kim, “Facilitating Effects of Emotion on the Perception of Biological Motion: Evidence for a Happiness Superiority Effect,” *Perception*, vol. 46, no. 6, pp. 679–697, 2017, doi: 10.1177/0301006616681809.

[52] F. Marmolejo-Ramos, A. Murata, K. Sasaski, Y. Yamada, A. Ikeda, J. A. Hinojosa, K. Watanabe, M. Parzuchowski, C. Tirado, and R. Ospina, “Your face and moves seem happier when I smile,” *Exp. Psychol.*, vol. 67, no. 1, pp. 14–22, 2020, doi: 10.1027/1618-3169/a000470.

[53] C. C. Carbon, M. J. Held, and A. Schütz, “Reading Emotions in Faces With and Without Masks Is Relatively Independent of Extended Exposure and Individual Difference Variables,” *Front. Psychol.*, vol. 13, 2022, doi: 10.3389/fpsyg.2022.856971.

[54] P. Ross and E. George, “Are face masks a problem for emotion recognition? Not when the whole body is visible.,” *Front. Neurosci.*, vol. 16, 2021, doi: 10.3389/fnins.2022.915927.

[55] L. Mason, F. Shix, T. Falck-Ytter, B. Chakrabarti, T. Charman, E. Loth, J. Tillmann, T. Banaschewski, S. Baron-Cohen, S. Bölte, J. Buitelaar, S. Durston, B. Oranje, A. M. Persico, C. Beckmann, T. Bougeron, F. Dell'Acqua, C. Ecker, C. Moessnang, D. Murphy, M. H. Johnson, E. J. H. Jones, and the LEAP Team, “Preference for biological motion is reduced in ASD: implications for clinical trials and the search for biomarkers,” *Mol. Autism*, vol. 12, no. 1, 2021, doi: 10.1186/s13229-021-00476-0.

[56] A. Freitas-Magalhães, “Facial Expression of Emotion,” in *Encyclopedia of Human Behavior*, 2nd ed., pp. 173–183, 2012, doi: 10.1016/B978-0-12-375000-6.00387-6.

[57] D. Purves, G. J. Augustine, D. Fitzpatrick, W. C. Hall, A. LaMantia, J O. McNamara, and S. M. Williams, *Neuroscience*, 3rd ed, 2019.

[58] D. Pitcher and L. G. Ungerleider, “Evidence for a Third Visual Pathway Specialized for

Social Perception," *Trends Cogn. Sci.*, vol. 25, no. 2, pp. 100–110, 2021, doi: 10.1016/j.tics.2020.11.006.

[59] J. V. Duarte, G. N. Costa, R. Martins, and M. Castelo-Branco, "Pivotal role of hMT+ in long-range disambiguation of interhemispheric bistable surface motion," *Hum. Brain Mapp.*, vol. 38, pp. 4882–4897, 2017, doi: 10.1002/hbm.23701.

[60] E. Grossman, M. Donnelly, R. Price, D. Pickens, V. Morgan, G. Neighbor, and R. Blake, "Brain areas involved in perception of biological motion," *J. Cogn. Neurosci.*, vol. 12, no. 5, pp. 711–720, 2000, doi: 10.1162/089892900562417.

[61] P. Neri, M. C. Morrone, and D. C. Burr, "Seeing biological motion," *Nature*, vol. 395, no. 6705, pp. 894–896, 1998, doi: 10.1038/27661.

[62] J. Thompson and R. Parasuraman, "Attention, biological motion, and action recognition," *Neuroimage*, vol. 59, no. 1, pp. 4–13, 2012, doi: 10.1016/j.neuroimage.2011.05.044.

[63] G. Johansson, "Visual perception of biological motion and a model for its analysis," *Percept. Psychophys.*, vol. 14, no. 2, pp. 201–211, 1973, doi: 10.3758/BF03212378.

[64] K. Alaerts, E. Nackaerts, P. Meyns, S. P. Swinnen, and N. Wenderoth, "Action and emotion recognition from point light displays: An investigation of gender differences," *PLoS One*, vol. 6, no. 6, 2011, doi: 10.1371/journal.pone.0020989.

[65] K. Steel, E. Ellem, and D. Baxter, "The application of biological motion research: biometrics, sport, and the military," *Psychon. Bull. Rev.*, vol. 22, no. 1, pp. 78–87, 2015, doi: 10.3758/s13423-014-0659-5.

[66] S. Runeson and G. Frykholm, "Kinematic specification of dynamics as an informational basis for person-and-action perception: Expectation, gender recognition, and deceptive intention," *J. Exp. Psychol. Gen.*, vol. 112, no. 4, pp. 585–615, 1983, doi: 10.1037/0096-3445.112.4.585.

[67] Y. Ma, H. M. Paterson, and F. E. Pollick, "A motion capture library for the study of identity, gender, and emotion perception from biological motion," *Behav. Res. Methods*, vol. 38, no. 1, pp. 134–141, 2006, doi: 10.3758/BF03192758.

[68] G. Mather, K. Radford, and S. West, "Low-level visual processing of biological motion," *Proc. R. Soc. B Biol. Sci.*, vol. 249, no. 1325, pp. 149–155, 1992, doi: 10.1098/rspb.1992.0097.

[69] N. F. Troje, "Decomposing biological motion: A framework for analysis and synthesis of human gait patterns," *J. Vis.*, vol. 2, no. 5, pp. 371–387, 2002, doi: 10.1167/2.5.2.

[70] D. H. F. Chang and N. F. Troje, "Perception of animacy and direction from local biological motion signals," *J. Vis.*, vol. 8, no. 5, pp. 1–10, 2008, doi: 10.1167/8.5.3.

[71] S. Quadflieg and K. Koldewyn, "The neuroscience of people watching: How the human

brain makes sense of other people's encounters," *Ann. N. Y. Acad. Sci.*, vol. 1396, pp. 166–182, 2017, doi: 10.1111/nyas.13331.

[72] J. Grèzes, P. Fonlupt, B. Bertenthal, C. Delon-Martin, C. Segebarth, and J. Decety, "Does perception of biological motion rely on specific brain regions?," *Neuroimage*, vol. 13, no. 5, pp. 775–785, 2001, doi: 10.1006/nimg.2000.0740.

[73] J. V. Duarte, R. Abreu, and M. Castelo-Branco, "A two-stage framework for neural processing of biological motion," *Neuroimage*, vol. 259, p. 119403, 2022, doi: 10.1016/j.neuroimage.2022.119403.

[74] S. Gilaie-Dotan, R. Kanai, B. Bahrami, G. Rees, and A. P. Saygin, "Neuroanatomical correlates of biological motion detection," *Neuropsychologia*, vol. 51, no. 3, pp. 457–463, 2013, doi: 10.1016/j.neuropsychologia.2012.11.027.

[75] M. M. De Wit and L. J. Buxbaum, "Critical Motor Involvement in Prediction of Human and Non-biological Motion Trajectories," *J. Int. Neuropsychol. Soc.*, vol. 23, no. 2, pp. 171–184, 2017, doi: 10.1017/S1355617716001144.

[76] L. Miller, H. C. Agnew, and K. S. Pilz, "Behavioural evidence for distinct mechanisms related to global and biological motion perception," *Vision Res.*, vol. 142, pp. 58–64, 2018, doi: 10.1016/j.visres.2017.08.004.

[77] D. H. F. Chang, H. Ban, Y. Ikegaya, I. Fujita, and N. F. Troje, "Cortical and subcortical responses to biological motion," *Neuroimage*, vol. 174, pp. 87–96, 2018, doi: 10.1016/j.neuroimage.2018.03.013.

[78] E. Dayan, A. Mukovskiy, Y. Douek, M. A. Giese, R. Malach, and T. Flash, "The Default Mode Network Differentiates Biological from Non-Biological Motion," *Cereb. Cortex*, vol. 26, no. 1, pp. 234–245, 2016, doi: 10.1093/cercor/bhu199.

[79] X. Di and B. B. Biswal, "Identifying the default mode network structure using dynamic causal modeling on resting-state functional magnetic resonance imaging," *Neuroimage*, vol. 86, pp. 53–59, 2014, doi: 10.1016/j.neuroimage.2013.07.071.

[80] L. Nummenmaa, K. Seppälä, and V. Putkinen, "Molecular imaging of the human emotion circuit," *PsyArXiv*, no. March, 2020, doi: 10.31234/osf.io/5w63q.

[81] M. R. Roxo, P. R. Franceschini, C. Zubaran, F. D. Kleber, and J. W. Sander, "The limbic system conception and its historical evolution," *ScientificWorldJournal.*, vol. 11, pp. 2427–2440, 2011, doi: 10.1100/2011/157150.

[82] K. O. Lövblad, K. Schaller, and M. Isabel Vargas, "The fornix and limbic system," *Semin. Ultrasound, CT MRI*, vol. 35, no. 5, pp. 459–473, 2014, doi: 10.1053/j.sult.2014.06.005.

[83] M. Catani, F. Dell'Acqua, and M. Thiebaut de Schotten, "A revised limbic system model for memory, emotion and behaviour," *Neurosci. Biobehav. Rev.*, vol. 37, no. 8, pp. 1724–

1737, 2013, doi: 10.1016/j.neubiorev.2013.07.001.

[84] T. Kamigaki, “Prefrontal circuit organization for executive control,” *Neurosci. Res.*, vol. 140, pp. 23–36, 2019, doi: 10.1016/j.neures.2018.08.017.

[85] B. D. Hare and R. S. Duman, “Prefrontal cortex circuits in depression and anxiety: contribution of discrete neuronal populations and target regions,” *Mol. Psychiatry*, vol. 25, no. 11, pp. 2742–2758, 220, doi: 10.1038/s41380-020-0685-9.

[86] R. K. Naumann, J. M. Ondracek, S. Reiter, M. Shein-Idelson, M. A. Tosches, T. M. Yamawaki, and G. Laurent, “The reptilian brain,” *Curr. Biol.*, vol. 25, no. 8, pp. R317–R321, 2015, doi: 10.1016/j.cub.2015.02.049.

[87] P. C. Schmid and M. Schmid Mast, “Mood effects on emotion recognition,” *Motiv. Emot.*, vol. 34, no. 3, pp. 288–292, 2010, doi: 10.1007/s11031-010-9170-0.

[88] E. A. Phelps, S. Ling, and M. Carrasco, “Emotion facilitates perception and potentiates the perceptual benefits of attention,” *Psychol. Sci.*, vol. 17, no. 4, pp. 292–299, 2006, doi: 10.1111/j.1467-9280.2006.01701.x.

[89] B. L. Fredrickson, “The role of positive emotions in positive psychology: The broaden-and-build theory of positive emotions,” *Am. Psychol.*, vol. 56, no. 3, pp. 218–226, 2001, doi: 10.1037/0003-066X.56.3.218.

[90] K. Gasper and G. L. Clore, “Attending to the big picture: Mood and global versus local processing of visual information,” *Psychol. Sci.*, vol. 13, no. 1, pp. 34–40, 2002, doi: 10.1111/1467-9280.00406.

[91] J. R. Huntsinger, G. L. Clore, and Y. Bar-Anan, “Mood and Global-Local Focus: Priming a Local Focus Reverses the Link Between Mood and Global-Local Processing,” *Emotion*, vol. 10, no. 5, pp. 722–726, 2010, doi: 10.1037/a0019356.

[92] D. Navon, “Forest before trees: The precedence of global features in visual perception,” *Cogn. Psychol.*, vol. 9, no. 3, pp. 353–383, 1977, doi: 10.1016/0010-0285(77)90012-3.

[93] P. Sarkheil, R. Goebe, F. Schneider, and K. Mathiak, “Emotion unfolded by motion: A role for parietal lobe in decoding dynamic facial expressions,” *Soc. Cogn. Affect. Neurosci.*, vol. 8, no. 8, pp. 950–957, 2013, doi: 10.1093/scan/nss092.

[94] G. Cristóbal, L. U. Perrinet, and M. S. Keil, *Biologically inspired computer vision: Fundamentals and applications*, 1st ed., 2015.

[95] M. A. Lindquist and T. D. Wager, "*Principles of functional Magnetic Resonance Imaging"*, New York: Leanpub, 2015.

[96] S. A. Huettel, A. W. Song, and G. Mccarthy, *Functional Magnetic Resonance Imaging*,3rd ed., 2014.

[97] K. Uludag, D. J. Dubowitz, R.B Buxton, “Basic Principles Of Functional MRI,” in

Clinical MRI, 2005, pp. 249-287.

[98] E. Amaro and G. J. Barker, "Study design in fMRI: Basic principles," *Brain Cogn.*, vol. 60, no. 3, pp. 220–232, 2006, doi: 10.1016/j.bandc.2005.11.009.

[99] D. H. Brainard, "The Psychophysics Toolbox," *Spat. Vis.*, vol. 10, no. 4, pp. 433–436, 1997.

[100] J. J. A. van Boxtel and H. Lu, "A biological motion toolbox for reading, displaying, and manipulating motion capture data in research settings," *J. Vis.*, vol. 13, no. 12, 2013, doi: 10.1167/13.12.7.

[101] R. C. Oldfield, "The assessment and analysis of handedness: The Edinburgh inventory," *Neuropsychologia*, vol. 9, no. 1, pp. 97–113, 1971, doi: 10.1016/0028-3932(71)90067-4.

[102] I. C. Galinha, C. R. Pereira, and F. Esteves, "Versão reduzida da escala de afeto positivo e negativo portuguesa - PANAS-Port-VR: Análise fatorial confirmatória e invariância temporal," *Psicologia*, vol. 28, no. 1, pp. 53–65, 2014, doi: 10.17575/rpsicol.v28i1.622.

[103] S. M. Smith, M. Jenkinson, M. W. Woolrich, C. F. Beckmann, T. E. J. Behrens, H. Johansen-Berg, P. R. Bannister, M. De Luca, I. Drobnjak, D. E. Flitney, R. K. Niazy, J. Saunders, J. Vickers, Y. Zhang, N. De Stefano, J. M. Brady, and P. M. Matthews, "Advances in functional and structural MR image analysis and implementation as FSL," *Neuroimage*, vol. 23, Suppl 1, pp. S208–S219, 2004, doi: 10.1016/j.neuroimage.2004.07.051.

[104] J. L. R. Andersson, S. Skare, and J. Ashburner, "How to correct susceptibility distortions in spin-echo echo-planar images: Application to diffusion tensor imaging," *Neuroimage*, vol. 20, no. 2, pp. 870–888, 2003, doi: 10.1016/S1053-8119(03)00336-7.

[105] R. M. Birn, J. B. Diamond, M. A. Smith, and P. A. Bandettini, "Separating respiratory-variation-related fluctuations from neuronal-activity-related fluctuations in fMRI," *Neuroimage*, vol. 31, no. 4, pp. 1536–1548, 2006, doi: 10.1016/j.neuroimage.2006.02.048.

[106] L. Kasper, S. Bollmann, A. O. Diaconescu, C. Hutton, J. Heinzle, S. Iglesias, T. U. Hauser, M. Sebold, Z. M. Manjaly, K. P. Pruessmann, and K. E. Stephan, "The PhysIO Toolbox for Modeling Physiological Noise in fMRI Data," *J. Neurosci. Methods*, vol. 276, pp. 56–72, 2017, doi: 10.1016/j.jneumeth.2016.10.019.

[107] S. Frässle, E. A. Aponte, S. Bollmann, K. H. Brodersen, C. T. Do, O. K. Harrison, S. J. Harrison, J. Heinzle, S. Iglesias, L. Kasper, E. I. Lomakina, C. Mathys, M. Müller-Schrader, I. Pereira, F. H. Petzschner, S. Raman, D. Schöbi, B. Toussaint, L. A. Weber, Y. Yao, and K. E. Stephan, "TAPAS: An Open-Source Software Package for Translational Neuromodeling and Computational Psychiatry," *Front. Psychiatry*, vol. 12, no. June, 2021, doi: 10.3389/fpsyt.2021.680811.

[108] H. J. Markowitsch, “Differential contribution of right and left amygdala to affective information processing,” *Behav. Neurol.*, vol. 11, no. 4, pp. 233–244, 1998, doi: 10.1155/1999/180434.

[109] E. A. Phelps, K. J. O’Connor, J. C. Gatenby, J. C. Gore, C. Grillon, and M. Davis, “Activation of the left amygdala to a cognitive representation of fear,” *Nat. Neurosci.*, vol. 4, no. 4, pp. 437–441, 2001, doi: 10.1038/86110.

[110] C. I. Wright, H. Fischer, P. J. Whalen, S. C. McInerney, L. M. Shin, and S. L. Rauch, “Differential prefrontal cortex and amygdala habituation to repeatedly presented emotional stimuli,” *Neuroreport*, vol. 12, no. 2, pp. 379–383, 2001, doi: 10.1097/00001756-200102120-00039.

[111] D. H. Zald and J. V. Pardo, “The neural correlates of aversive auditory stimulation,” *Neuroimage*, vol. 16, no. 3 I, pp. 746–753, 2002, doi: 10.1006/nimg.2002.1115.

[112] J. Gläscher and R. Adolphs, “Processing of the Arousal of Subliminal and Supraliminal Emotional Stimuli by the Human Amygdala,” *J. Neurosci.*, vol. 23, no. 32, pp. 10274–10282, 2003, doi: 10.1523/jneurosci.23-32-10274.2003.